Intrusion and deformation at Campi Flegrei, southern Italy: Sills, dikes, and regional extension

Judith Y. L. Woo[1] and Christopher R. J. Kilburn[1]

[1]   The Campi Flegrei volcanic district, in southern Italy, has been uplifted since 1968 by a net maximum of 3 m during the intervals 1968–1972 and 1982–1984. The uplift represents a permanent deformation against a background rate of subsidence of about 17 mm a^{-1}. Previous models have reproduced the observed vertical deformation but not the full pattern of horizontal movements. The 1982–1983 deformation is here reanalyzed in terms of a penny-shaped sill on its own, with a tabular surface protrusion, or in an extensional stress field. It can be explained best by the intrusion of a sill (of 0.03–0.04 km^3 at a depth of 2.75 km) in a crust that is being stretched ESE-WNW at a strain rate of about $5.6 \times 10^{-5} a^{-1}$. The sill's volume is similar to the common volumes of Campi Flegrei's eruptions since the Neapolitan Yellow Tuff (NYT) caldera was formed 15.6 ka ago. This similarity and the permanent nature of the uplift favor magmatic intrusion as the primary source of unrest. Sill formation may thus reflect the spreading of magma at a level of neutral buoyancy or along lateral discontinuities in the crust. The southern part of the caldera has been shielded from post-NYT eruptions, despite some 33 m of permanent uplift since Roman times. Precursors to eruptions may thus be related not to caldera-wide uplift but to the preceding conditions that determine whether magma ascends beneath the southern part of the caldera (favoring sill intrusion) or elsewhere (favoring an eruption).

1.   Introduction

[2]   Campi Flegrei is a volcanic field that covers about 200 km^2 along the coast immediately west of Naples in southern Italy (Figures 1 and 2). It is dominated geophysically by a caldera, 6–7 km across, produced about 15.6 ka BP during the eruption of the 40 km^3 Neapolitan Yellow Tuff or NYT [*Deino et al.*, 2004]. Eruptions following the NYT event have been smaller (0.01–1 km^3) and from predominantly monogenetic centers across the district [*Di Girolamo et al.*, 1984; *Lirer et al.*, 1987; *Rosi and Sbrana*, 1987].

[3]   The caldera has undergone vertical movements (both uplift and subsidence) of tens of meters for at least 5000 years [*Cinque et al.*, 1985; *Bellucci et al.*, 2006]. Most recently, the inner 100 km^2 of the district have been subject to episodes of major unrest, in 1968–1972 and 1982–1984, which together have produced a net maximum uplift of 3 m [*Corrado et al.*, 1977; *Berrino et al.*, 1984; *Bellucci et al.*, 2006]. The uplifts were centered about 1 km east of the old port of Pozzuoli (Figures 1 and 2) [*Bianchi et al.*, 1987]. They ended 430 years of subsidence [*Berrino et al.*, 1984]

and were accompanied by volcano-tectonic (VT) earthquakes with typical magnitudes of 0–2 but a maximum of 4 [*Aster and Meyer*, 1988; *De Natale et al.*, 1995]. In both cases, the VT seismicity and concern about an eruption triggered the evacuation of as many as 40,000 people from the Pozzuoli district [*Barberi et al.*, 1984].

[4]   Analyses of the post-1968 uplifts have focused on the 1982–1984 episode, because this is the episode for which deformation data are more tightly constrained. The data indicate an approximately radial pattern of vertical deformation, and as a result, most analyses have attributed deformation to an axisymmetric pressure source at depths between 2 and 5.5 km (see Table 1 and references therein). On their own, however, axisymmetric pressure sources favor a radial symmetry also in the pattern of horizontal deformation. Such symmetry was not observed during the 1982–1984 unrest, for which horizontal deformation more than 2 km from the center of uplift decays more rapidly to the north, compared with behavior to the east and west [*Bianchi et al.*, 1987]; movements to the south remain unrecorded because they occurred offshore.

[5]   This paper incorporates the distal horizontal data to show that the full pattern of deformation can be explained by an axisymmetric sill within an ESE-WNW extensional stress field. The preferred values for sill location, dimensions, and depth confirm the results from previous sill models that used an alternative data set [*Dvorak and Berrino*, 1991; *Battaglia*

[1]Aon Benfield UCL Hazard Research Centre, Department of Earth Sciences, University College London, London, UK.
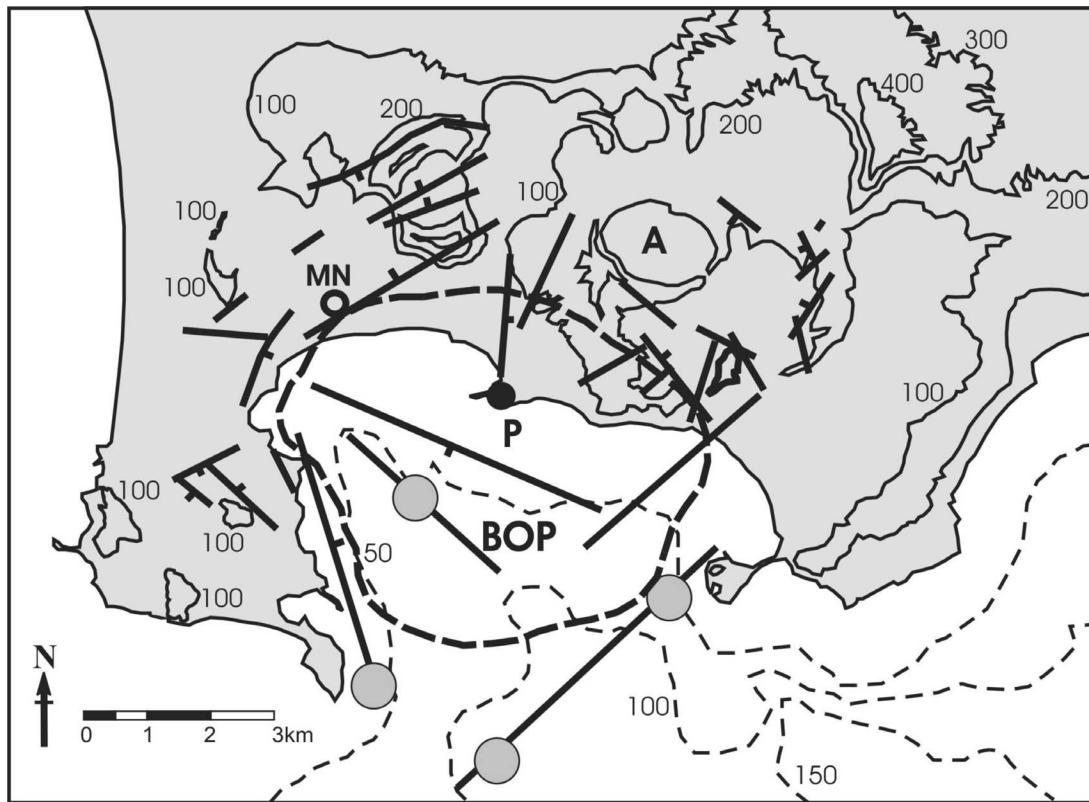
Figure 1. Campi Flegrei is a flat-lying volcanic district bounded by the sea to the west and south and by elevations of typically less than 300 m above sea level to the north and east. Offshore, the sea floor deepens gently southwards to 100 m across the mouth of the Bay of Pozzuoli (BOP). Primary faults (solid lines) tend to be oriented as conjugate pairs trending NW-SE and NE-SW, as well as ENE-WSW and ESE-WNW (ticks show downthrow direction). Most of the Neapolitan Yellow Tuff (NYT) caldera (large dashes) lies offshore in the Bay of Pozzuoli. The caldera rim is taken from *Barberi et al.* [1991], who defined its location by a negative gravity anomaly rather than by topography or bathymetry. The solid circles offshore show the locations of buried volcanic structures inferred from marine seismic reflection data and which predate the formation of the NYT caldera [*Bruno*, 2004]. The town of Pozzuoli (P) lies on the coast just inside the northern rim of the NYT caldera. The distribution of post-NYT cones is better shown by the digital terrain maps in Figure 2. The cones of Astroni (A) and Monte Nuovo (MN) are shown as reference locations to connect with Figure 2. Naples lies to the east, beyond the right margin. Topographic and bathymetric contours are given in meters. (Data from *Barberi et al.* [1991], *Di Vito et al.* [1999], and *Bruno* [2004].) A 1:15,000 geological map is available in the study by *Rosi and Sbrana* [1987].

et al., 2006; *Amoruso et al.*, 2008], whereas the introduction of an external stress field yields a first-order improvement on those analyses. Combined with long-term patterns of ground movement at Campi Flegrei [*Bellucci et al.*, 2006], the results favor magma as the primary source for sill development and identify new constraints on magmatic and tectonic contributions to caldera unrest.

2. Structure and Recent Deformation of Campi Flegrei

[6] Campi Flegrei lies within a graben, at least 30 km wide, between the Apennines and the Tyrrhenian coast (Figure 3). The length of the graben is defined by regional NE-SW trending faults near mounts Massico and the Sorrento peninsula, respectively 35 km NNW and 30 km SSE of Campi Flegrei [*Cassano and La Torre*, 1987;

Scandone et al., 1991; *Acocella et al.*, 1999]. During the Holocene, the region has been subjected to a tectonic ESE-WNW extension [*Milia et al.*, 2009], combined with the NE-SW spreading of the Apennine mountains [*Roberts*, 2006; *Papanikolaou and Roberts*, 2007].

[7] Geophysical data have identified an area of major subsidence about 6–7 km across beneath Campi Flegrei and the Bay of Pozzuoli [*Barberi et al.*, 1991; *Zollo et al.*, 2003]. Interpreted as a caldera produced during the NYT eruption (Figure 1), the zone of collapse has since been filled with volcanic deposits and so is not clearly defined by modern surface topography [*Barberi et al.*, 1991]. It is conventionally postulated that the NYT caldera represents a second episode of collapse, following an initial episode during eruption of the Campanian Ignimbrite (CI) about 39 ka B.P. [*Rosi et al.*, 1983; *Barberi et al.*, 1991; *Orsi et al.*, 1999]. However, recent geological studies suggest that the CI may
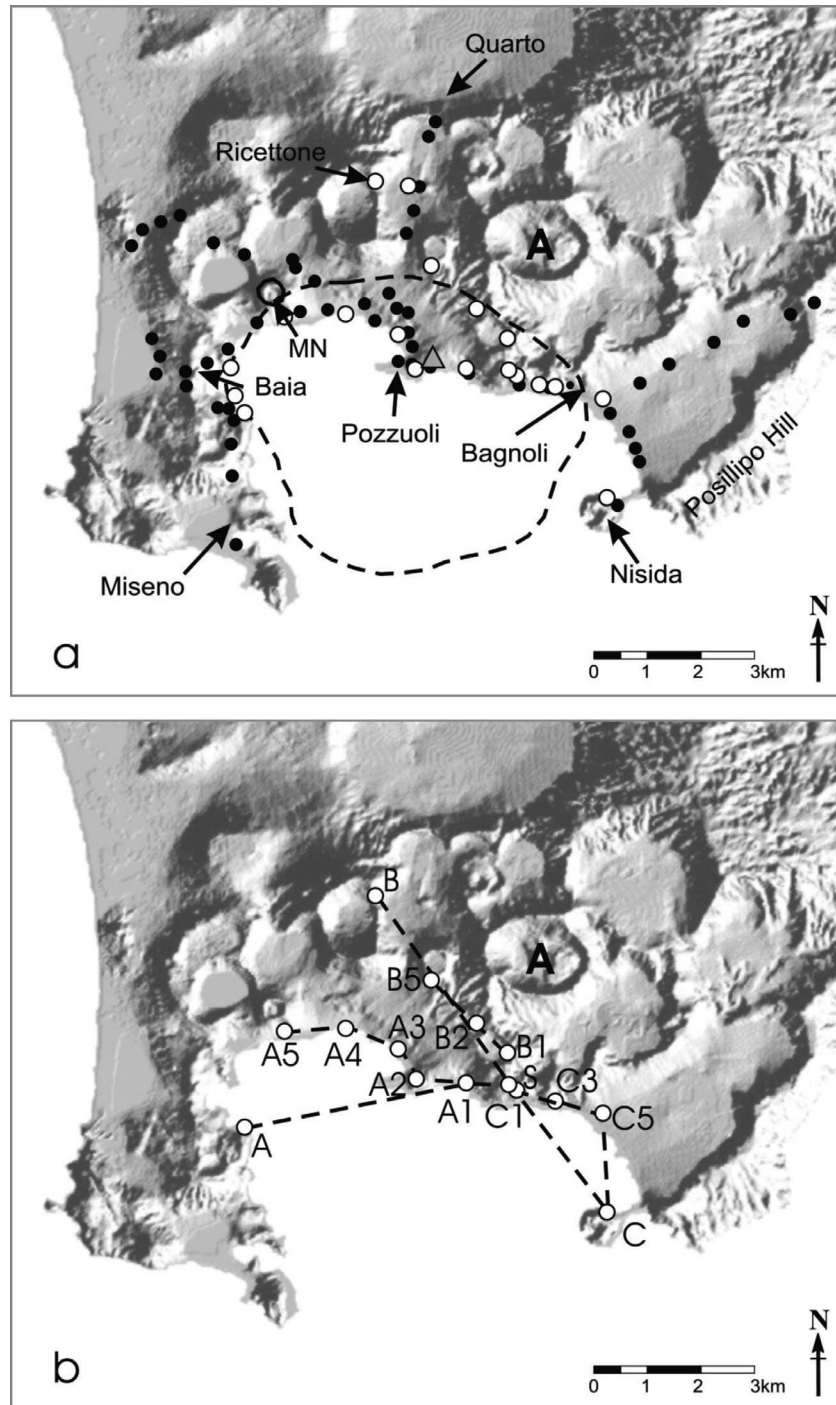
Figure 2. (a) The post-NYT eruptions have produced a collection of cones mainly to the north and west of the NYT caldera (large dashes). The last eruption, in 1538, produced Monte Nuovo (MN), about 3 km WNW of Pozzuoli. The June 1982 to June 1983 data were obtained from leveling stations (black circles), for vertical deformation, and electronic distance measuring stations (white circles) for horizontal deformation. The triangle east of Pozzuoli shows the center of deformation to which the measurements are referred. (Data from *Berrino et al.* [1984] and *Bianchi et al.* [1987].) (b) The horizontal measurements for the September 1980 to September 1983 data set were obtained as movements between selected stations, as well as movements between three distal stations (A, B, C) to station S (dashed lines). The Astroni crater (A in bold) is also shown as a location reference for comparing with Figure 1. (Data from *Dvorak and Berrino* [1991].)

Table 1. Parameters for Selected 3-D Elastic Deformation Models for Campi Flegrei, 1982–1984

Period (for Vertical Deformation Measurements)	Source Depth f (km)	Radius a (km)	Best Fit Source Model	Overpressure ΔP (MPa)	Crustal Rigidity μ (GPa)	Reference
Jan. 1982 to June 1984	2.8	0.3[a]	Point (Mogi model)	2700[a]	5	*Berrino et al.* [1984]
June 1982 to June 1983	5.5	1.5 × 0.75	Oblate spheroid	30	4.8 (0.1–30 for heterogeneous crustal model)	*Bianchi et al.* [1987]
Jan. 1981 to Sept. 1983	2.8	3.0 × 1.5	Rectangular sheet	13?	?	*Dvorak and Berrino* [1991]
Jan. 1982 to Dec. 1984 ?	5	1	Sphere and ring faults with radii of 2 and 4 km	75	5	*Orsi et al.* [1999]
June 1982 to June 1983	5	1	Sphere with ring faults	100	5	*De Natale et al.* [2001]
Jan. 1982 to Dec. 1984 ?	4.5	1	Sphere and ring fault at rim of NYT	35	5	*Beauducel et al.* [2004]
Jan. 1982 to June 1984	5	0.8	Sphere	40–50	3–6.5 (elasto-plastic crust)	*Trasatti et al.* [2005]
1982–1983	2.9	2.2 × 1.4	Vertical prolate spheroid	52	10	*Gottsmann et al.* [2006][b]
Sept. 1980 to Sept. 1983	2.6	2.4	Penny-shaped sill	3	5	*Battaglia et al.* [2006]
Jan. 1982 to June 1984	2 and 5.3	0.1 and 0.2	Two spheres and ring fault with radius of 2.5 km	30 in both	10	*Folch & Gottsmann* [2006]
Sept. 1980 to Sept. 1983	3.1	2.7	Penny-shaped sill	15 (For a single μ of 15 GPa)	Layered crust μ increases with depth from 1.3 to 27 GPa (at 4 km)	*Amoruso et al.* [2008]

[a]Sample values from result $\Delta P = 6.4 \times 10^{16}/a^3$, ΔP in Pascals, and a in meters.
[b]This source appears to give a good fit to both the horizontal and vertical patterns of deformation described by *Bianchi et al.* [1987]. However, in order to fit the horizontal data (assumed to be radially symmetric), the locations for the vertical deformation data points have been shifted toward the center by about 500 m with respect to the locations in the study by *Bianchi et al.* [1987]. The reasons for this shift are unclear.

instead have been fed from fissures north of Campi Flegrei [*Rolandi et al.*, 2003]. Whether or not the CI collapse is confirmed, the most prominent geophysical structure in Campi Flegrei remains the NYT caldera.

[8] Pozzuoli, near the center of recent uplift, lies in the northern third of the NYT caldera; to the south, most of the remaining two thirds of the caldera lies offshore in the Bay of Pozzuoli (Figures 1 and 2). As summarized in the study by *Zollo et al.* [2008], gravity, seismic-tomographic, and borehole data [*Cassano and La Torre*, 1987; *Rosi and Sbrana*, 1987; *Zollo et al.*, 2008] indicate that the upper 8.5 km of crust consists of (1) tuffs and massive lava to depths of 3 km; (2) a zone of thermally metamorphosed volcanic products and nonvolcanic rock, including silt and marl with a top at about 3.0 km beneath the NYT caldera, underlain by inferred basement carbonate rock; and (3) a zone rich in magma at depths between about 7.5 and 8.5 km. With a resolution of 1 km, the 2001 tomographic surveys have not detected molten bodies at depths of less than 7.5 km [*Zollo et al.*, 2003]. Any shallow magma intrusion, therefore, must either have solidified before the survey took place in September 2001 [*Zollo et al.*, 2008] or have a characteristic dimension (diameter for an equidimensional body or thickness for a dike or sill) of less than 1 km.

[9] At least 56 eruptions have occurred since the NYT event, the most recent of which produced Monte Nuovo in 1538, after a repose interval of about 3.3 ka [*Di Vito et al.*, 1999]. Previous eruptions appear to have been clustered between the NYT event and 9.5, 8.6–8.2, and 4.8–3.8 ka B. P. [*Di Vito et al.*, 1999]. Although the full range of erupted volumes covers 0.01–1 km^3, some 45%–50% have been smaller than 0.1 km^3 [*Lirer et al.*, 1987]. The magmas are typically trachytes and alkali trachytes, although subsidiary amounts of latites and phonolites have also been erupted [*Di Girolamo et al.*, 1984; *Rosi and Sbrana*, 1987; *D'Antonio et al.*, 1999]. The NYT itself is predominantly trachytic but contains minor amounts of less-evolved magmas, including latites [*Orsi et al.*, 1992; *Mastrolorenzo and Pappalardo*, 2006]. By extrapolation, therefore, the compositions of the buried tuffs and lavas are expected also to be dominated by trachytes and alkali-trachytes [*Rosi and Sbrana*, 1987].

[10] The post-NYT vents are located on the landward side of Campi Flegrei. The majority are found outside the rim of the NYT caldera, except along the Pozzuoli coastline, where eruptions have occurred within the northern one third of the caldera (Figure 2). No evidence for post-NYT eruptions has been found within the two thirds of the caldera that lies offshore, where the caldera is deepest [*Cassano and*
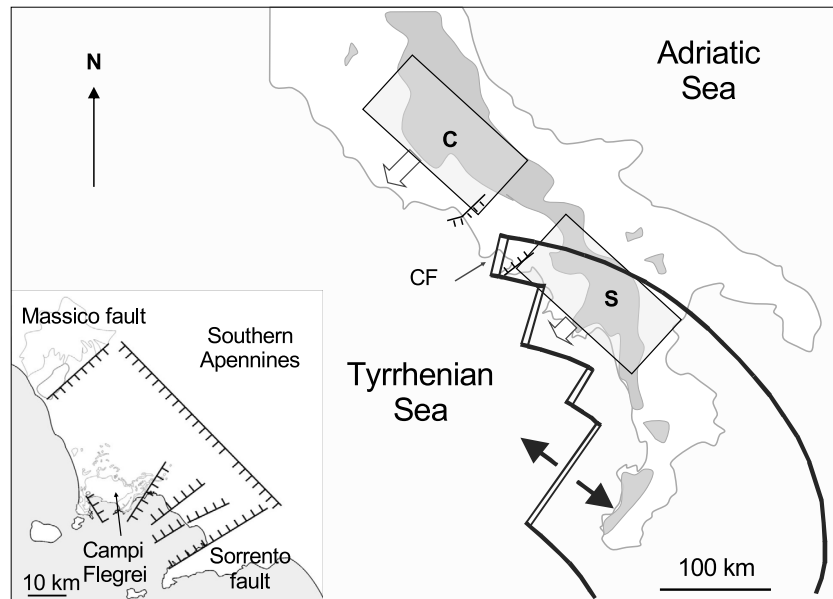
Figure 3. The Campanian Plain, which includes Campi Flegrei (CF), is bounded by the Massico and Sorrento faults (inset). For the past 0.7 Ma, tectonic movements have favored the relative SE displacement of the Tyrhennian side of Italy (bounded by the thick black curve), which has in part been accommodated by ESE-WNW extensions of segments, including Campi Flegrei (opening shown by the double black lines). The tectonic segments have been taken from *Milia et al.* [2009]. In addition, for the past 12–18 ka, the central (C) and southern (S) Apennines have been extending at mean rates of, respectively, 4.4 m (over 30–40 km) and 1.1 m (over 45 km) per thousand years, yielding mean strain rates of about 10^{-4} and 0.25×10^{-4} ka^{-1} [*Roberts*, 2006; *Papanikolaou and Roberts*, 2007]. Associated differential shearing along the Massico and Sorrento faults would additionally favor a net E-W extension across the Campanian Plain, including Campi Flegrei.

La Torre, 1987]. However, seismic reflection data suggest that vents did form in this area before the NYT caldera collapse (Figure 1) [*Bruno*, 2004]. The lack of post-NYT vents offshore may thus indicate an increased difficulty in magma ascent to the surface following caldera collapse.

[11] Since at least Roman times, Campi Flegrei has been subsiding at a mean rate of about 17 mm a^{-1} near Pozzuoli, with rates becoming smaller at increasing distances from the port [*Dvorak and Mastrolorenzo*, 1991; *Bellucci et al.*, 2006]. This secular subsidence has been interrupted by net uplift during three intervals (Figure 4): (1) for about 100 years before the 1538 eruption; (2) for 100 years or more at some time between 600 and 1200 A.D., but without an eruption; and (3) since 1968. After the secular rate of subsidence has been removed (Figure 4), the episodes of uplift are seen to have raised Pozzuoli cumulatively by some 33 m [*Bellucci et al.*, 2006].

[12] The post-1968 movements have been dominated by uplifts across Campi Flegrei between late 1968 and December 1972 and between June 1982 and December 1984 [*Berrino et al.*, 1984; *Bianchi et al.*, 1987; *Orsi et al.*, 1999]. Both were characterized by radial patterns of vertical deformation, which decayed from a maximum value near Pozzuoli to only a few percent of the maximum about 6 km away (Figure 5). At Pozzuoli itself, the corrected uplift (after subtracting the secular rate of subsidence) has shown net displacements of 1.7 and 1.8 m during 1968–1972 and 1982–1984 (Figure 5). After 1984, the surface subsided by 0.5 m before its rate had returned in 2000 to the equilibrium

secular value. The net uplift at Pozzuoli has thus been 1.3 m since 1982 and 3 m since 1968 (Figure 5).

[13] In addition to the major uplifts, Pozzuoli has undergone four mini-uplifts of 0.01–0.1 m between 1989 and 2007 [*Gaeta et al.*, 2003; *Saccarotti et al.*, 2007; *Troise et al.*, 2007]. The movements have been recorded by precise leveling and GPS surveys and, since 1992, also by interferometric methods [*Avallone et al.*, 1999; *Lanari et al.*, 2004]. The mini-uplifts developed over months to years, and the deformation subsequently relaxed over intervals of years without permanent deformation with respect to the secular trend [*Troise et al.*, 2007]. The temporary nature of the mini-uplifts suggests that they may have been the result of short-term changes in fluid flow through shallow aquifers 2007 [*Gaeta et al.*, 2003; *Saccarotti et al.*, 2007; *Troise et al.*, 2007]. A similar mechanism may also account for the nonequilibrium subsidence of 0.5 m during 1985–2000 [*Battaglia et al.*, 2006; *Troise et al.*, 2007]. In contrast, the permanent nature of the net 33 m uplift at Pozzuoli since Roman times suggests the action of magma intrusion and solidification at shallow depths [*Bellucci et al.*, 2006]. Indeed, the two major uplifts since 1968 have conventionally been attributed to the intrusion of magma (see references in Table 1), although changes in aquifer conditions have also been postulated [e.g., *Todesco et al.*, 2004; *Battaglia et al.*, 2006; *De Natale et al.*, 2006; *De Vivo and Lima*, 2006; *Bodnar et al.*, 2007; *Lima et al.*, 2009]. The present study makes no a priori assumptions about the type
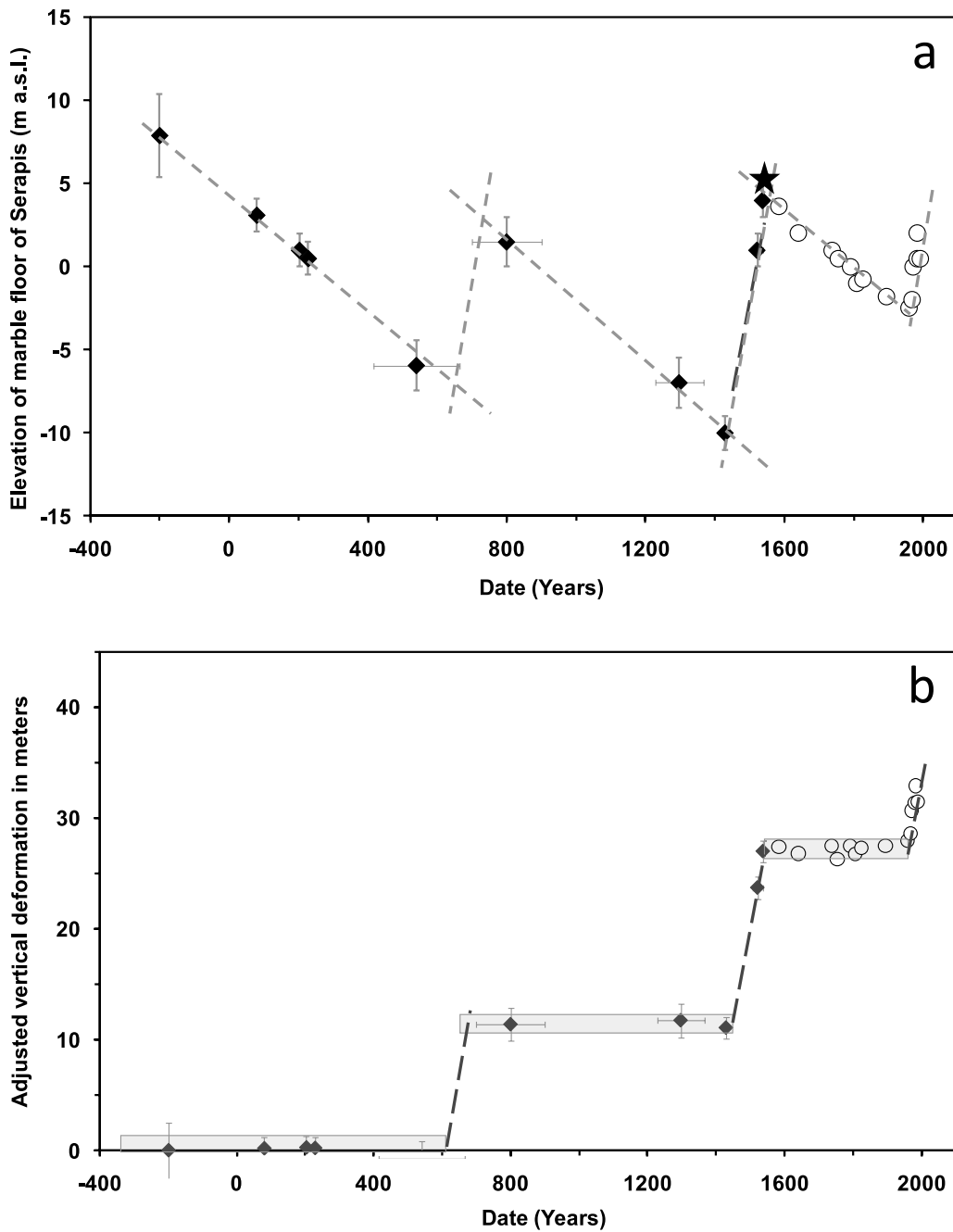
Figure 4. (a) Vertical movements of the Serapis market place in Pozzuoli indicate that two major uplifts have interrupted a general pattern of subsidence between Roman Times and 1968; another episode of major uplift may currently be in progress. The mean rates used here are 150 mm a^{-1} for uplift and 17 mm a^{-1} for subsidence. The 1538 eruption (star) occurred at the end of the second period of uplift. (b) Subtraction of the mean rate of subsidence reveals a steplike pattern of uplift. The two episodes before 1968 produced a permanent uplift of 30 m; the current uplift has increased this amount by 3 m (Figure 5). The location of the Serapis has been obtained from archaeological data and historic descriptions (diamonds), as well as direct geodetic measurements (open circles) (after *Bellucci et al.* [2006]).

of fluid in the deforming source, although the results yield additional constraints that interpretations must satisfy.

3. Rationale for Developing Sill Models to Interpret Deformation

3.1. Features Consistent With a Sill as a Pressure Source

[14] The primary condition that favors a sill-like geometry for the source of recent deformation in Campi Flegrei is that,

compared with alternative source geometries, sills require lower overpressures to produce the observed vertical deformation (Table 1). For a shallow, small-volume intrusion to remain stable without inducing bulk failure in the overlying crust, source overpressures cannot exceed the tensile strength of the uppermost crust σ_T by an amount $\Delta\sigma$ sufficient to drive the pressurized fluid into an opening fracture. High-temperature experiments on basalt indicate values of σ_T ~10 MPa at 25°C and 3–5 MPa at 900°C [*Rocchi et al.*, 2004]. Values for tuffs are expected to be
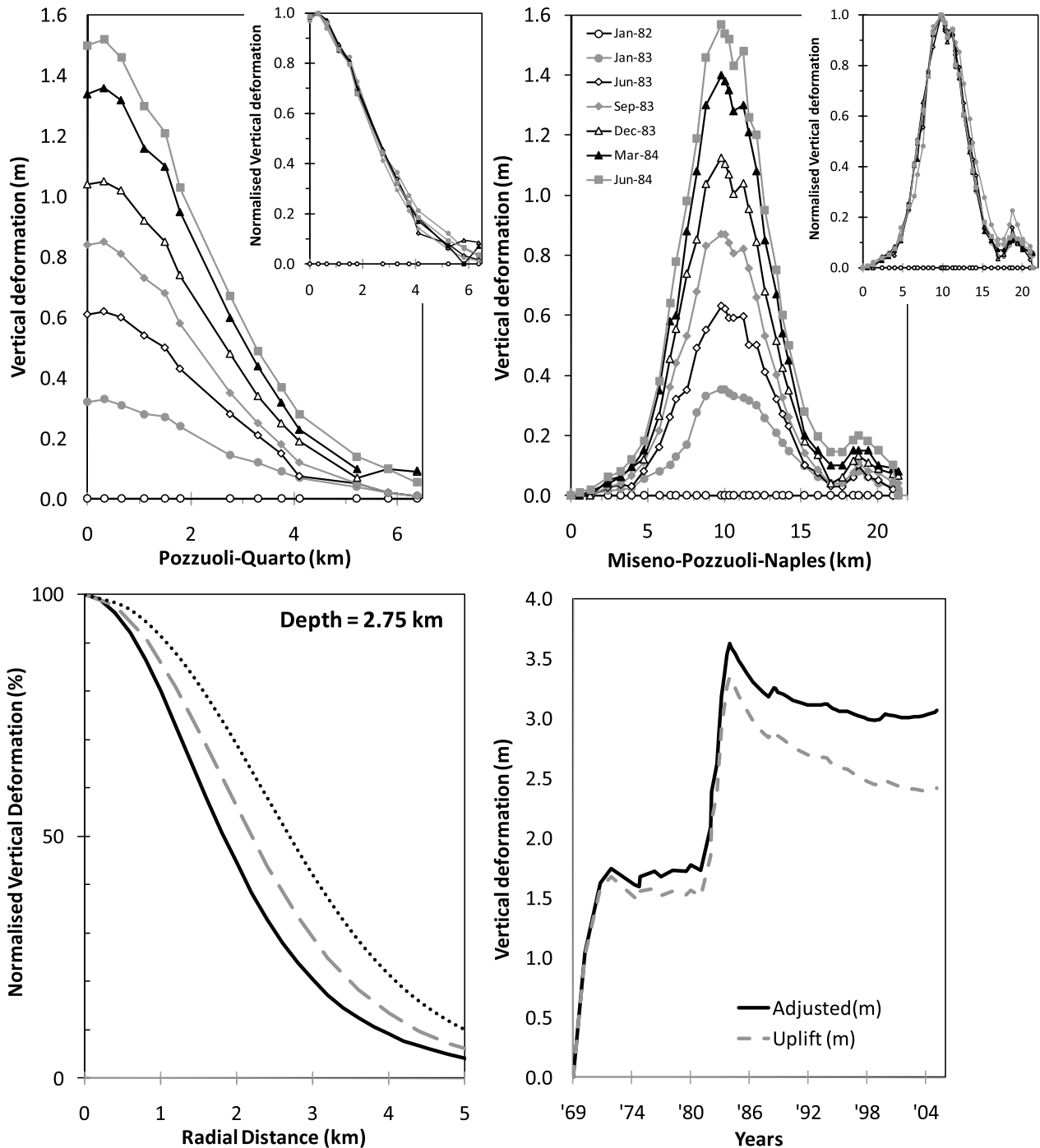

Figure 5

similar or smaller. The bulk tensile strength of the uppermost crust is thus expected to be on the order of MPa. Following *Rubin* [1995] and *Jellinek and DePaolo* [2003], the maximum value of $\Delta\sigma$ increases with the viscosity of the pressurized fluid, whether magma or water. The viscosity of magma is several orders of magnitude larger than aqueous fluids. If the source contains magma, $\Delta\sigma$ is expected to be on the order of MPa, assuming maximum magma viscosities of 10^5 Pa s for the typical trachytic to alkali-trachytic compositions erupted at Campi Flegrei [*Wohletz et al.*, 1995]; if the source contains water, $\Delta\sigma$ will be much smaller than σ_T. To a first approximation, therefore, an intrusion is not expected to break the overlying crust provided its overpressure does not exceed about 10 MPa. As shown in Table 1, only a sill-like geometry is able to reproduce the observed patterns of vertical deformation at suitably low overpressures.

3.2. Limits to Previous Sill Models Applied to the 1982–1984 Unrest

[15] The first study to consider a sill as a pressure source beneath Campi Flegrei appears to have been the two-dimensional analysis of the 1968–1972 unrest by *Bonasia et al.* [1984]. However, 3-D sill analyses have been applied only to the 1982–1984 unrest. Thus, *Dvorak and Berrino* [1991] modeled the pressure source as a rectangular sheet (Table 1), whereas *Battaglia et al.* [2006] and *Amoruso et al.* [2008] applied the penny-shaped source model of *Fialko et al.* [2001] for, respectively, a rheologically homogeneous and horizontally layered crust.

[16] All three models provide a good fit to the vertical deformation (Table 1). Applied to horizontal deformation, they also provide a good fit to movements east of Pozzuoli and broadly follow the observed trend in movement to the west (Figure 6). However, they provide a less-convincing fit to movements north of Pozzuoli, where they yield a smaller decay with distance than is observed (Figure 6).

[17] The three models also yield a restricted range in the preferred depth of between 2.6 and 3.1 km and, for the penny-shaped sills, a preferred radius of 2.4–2.7 km (Table 1). The depths are within 20% of each other and the penny-shaped radii within 12.5%. The differences are remarkably small given the assumptions in the three analyses. The similar depths indicate an insensitivity to the detailed geometry assumed for the sill, whereas the similar depths and dimensions of the two penny-shaped sills indicate

an insensitivity to the particular rheological structure that was assumed for the crust.

[18] Together, the results from the previous studies suggest (1) that a sill-like pressure source may be an important component in determining the pattern of deformation and (2) that the assumption of a rheologically homogeneous crust is a legitimate approximation until new rheological data to the contrary become available. Indeed, as shown in Appendix A, seismic-tomographic models of Campi Flegrei's crust lead to the same conclusion.

4. Data and Constraints on Modeling the 1982–1984 Deformation at Campi Flegrei

4.1. The Deformation Network

[19] The geodetic network in Campi Flegrei follows three lines radiating from Pozzuoli (Figure 2). Two of the lines run along the coast: (1) approximately WNW for 3 km to Monte Nuovo before curving south another 5.5 km to Miseno, about 5 km SW of Pozzuoli; and (2) an approximately ESE line that runs almost 5.5 km toward Posillipo, with one end station displaced 2.3 km southward at Nisida, 4 km SE from Pozzuoli. The third line runs inland, just west of north, about 4.4 km toward Quarto. Although data for vertical deformation are available for the entire network, measurements of horizontal deformation cover Pozzuoli-Ricettone on the Quarto line and (1) along the western line to just South of Baia, about 4.1 km WSW of Pozzuoli, and (2) along the eastern line to Bagnoli, 3 km ESE of Pozzuoli (Figure 2). Excluding measurements at Nisida, therefore, the horizontal data refer to lines directed broadly to the west, north, and ESE of Pozzuoli.

4.2. Data for Vertical Deformation

[20] Geodetic data were obtained by precise-leveling and dry-tilt measurements and are summarized in the studies by *Berrino et al.* [1984], *Bianchi et al.* [1987], and *Orsi et al.* [1999]. They contain an ambiguity in dating the onset of uplift. First, measurements from a tide gauge in Pozzuoli suggest that uplift began in June 1982 [*Berrino et al.*, 1984, Figure 6, and *Bianchi et al.*, 1987, Figure 2]. Second, geodetic data from the caldera-wide network reference vertical displacements to January 1982, with the following two sets of measurements being dated at January and June 1983 (Figure 5 in this paper, Figure 9 in the study by *Berrino et al.* [1984], and Figure 3 in the study by *Bianchi et al.* [1987]). Finally, the data set that has been used for

Figure 5. (top) Vertical deformation between January 1983 and June 1984 across Campi Flegrei, along the three principal measuring lines, (top left) from Pozzuoli (0 km) to Quarto and (top right) from Pozzuoli (10 km) to Miseno (0 km) and to Naples (20 km) [*Berrino et al.*, 1984]. The data at zero displacement (white circles) refer to reference measurements from January 1982; the remaining sets of six curves are for January 1983, June 1983, and then at intervals of 3 months until June 1984. Along all three directions, significant uplift begins about 5 km from Pozzuoli, independent of the time interval chosen; this is particularly evident when comparing the normalized patterns (insets). These show only minor changes compared with those expected (bottom left) from a sill increasing in radius from 1 to 3 km (solid, 1 km; large dash, 2 km; small dash, 3 km). Deformation may therefore have been dominated by thickening of the sill. (bottom right) Adjusted vertical displacement at Serapis between 1969 and 2005 (upper curve), after subtracting a background rate of subsidence of 17 mm a^{-1} from the measured deformation (lower curve) [*Bellucci et al.*, 2006]. The adjusted curve indicates that no significant movements occurred between 1972 and 1982, and that, by about 2000, the 1982–1984 uplift (of 1.8 m) had decayed by about 0.5 m to a new equilibrium level. The permanent deformation is consistent with two magma intrusions (1968–1972 and 1982–1984), whereas the 0.5 m decay may reflect the dissipation of fluids from disturbed aquifers.
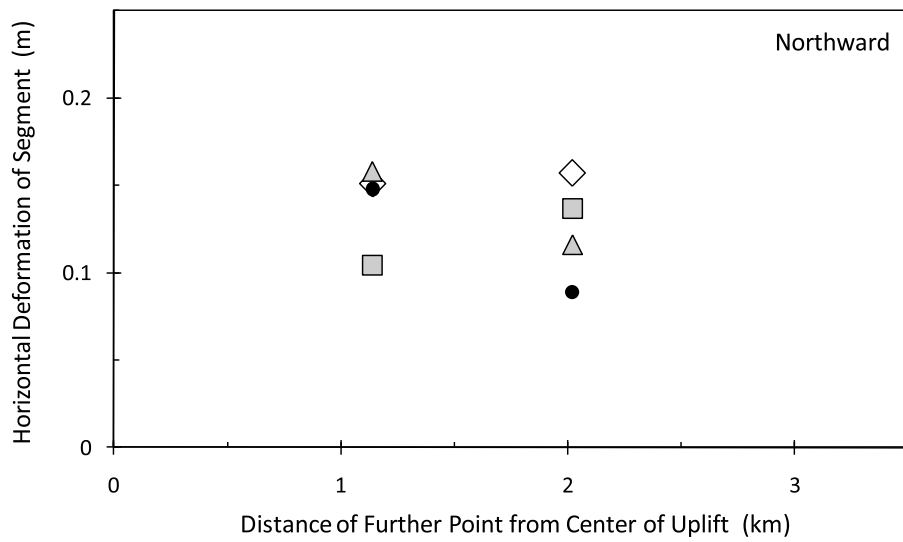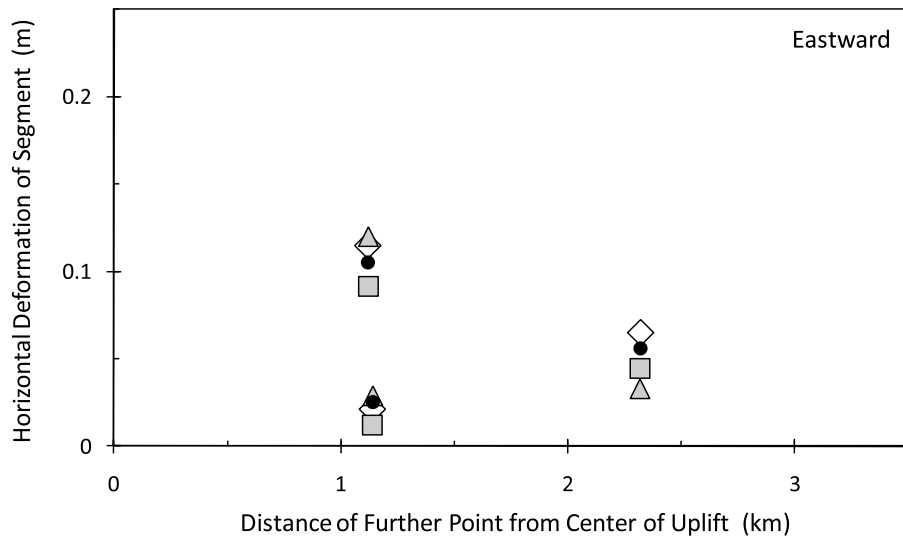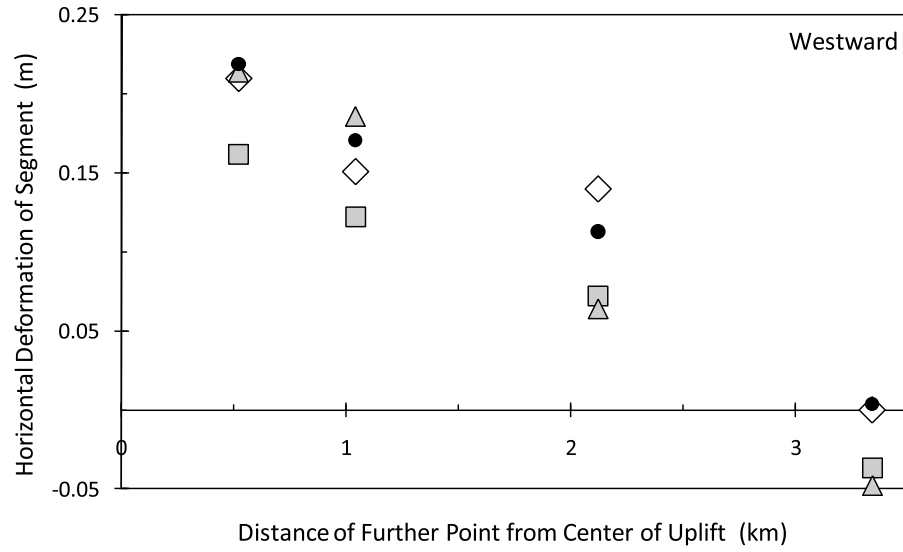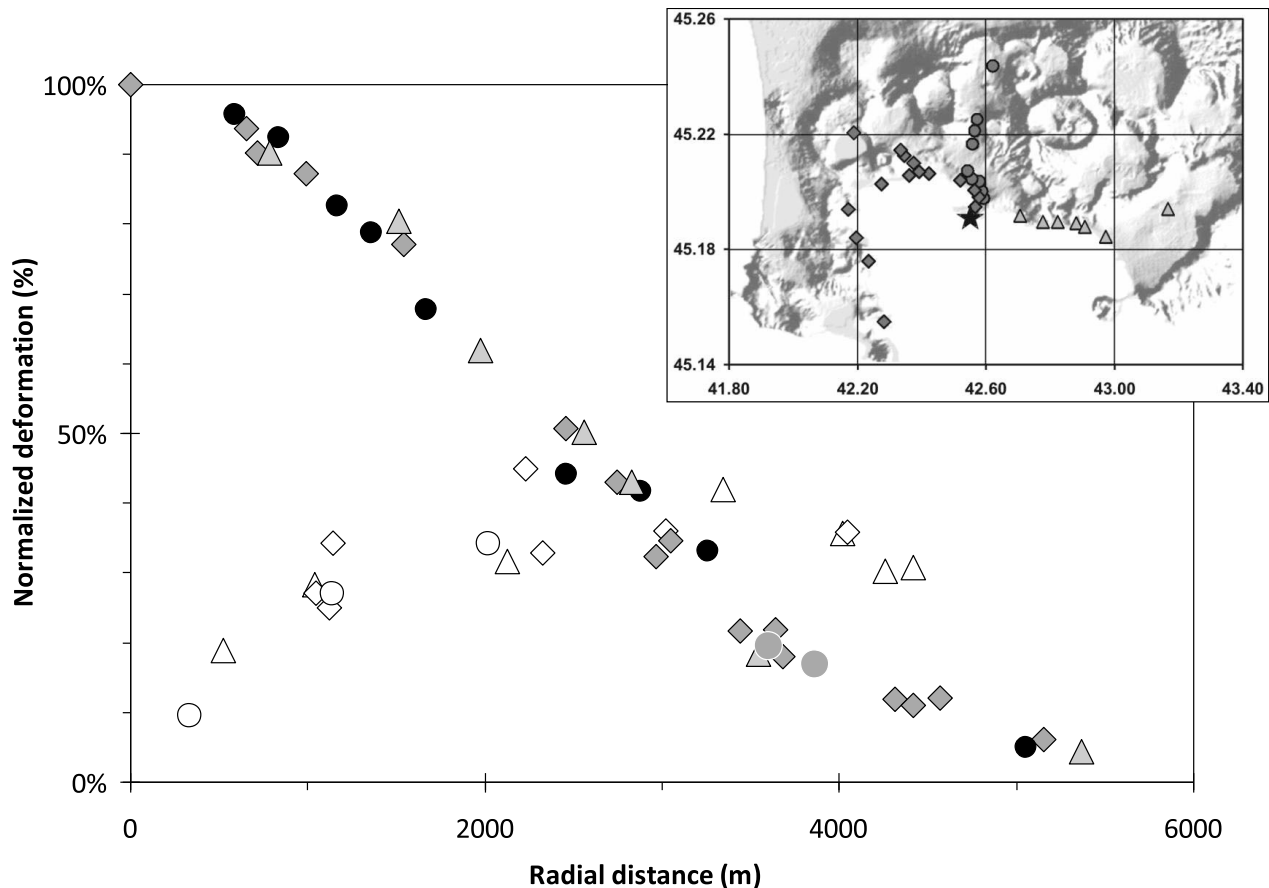
Figure 6

Figure 7. Patterns of vertical (solid symbols) and horizontal (white symbols) deformation recorded along all three measuring lines between June 1982 and June 1983 [*Bianchi et al.*, 1987]. As shown in the inset, triangles refer to the eastward Pozzuoli-Bagnoli line, diamonds refer to the westward Pozzuoli-Baia-Miseno line, and circles to the northward Pozzuoli-Ricettone line. Movements have been normalized against the maximum vertical deformation of 0.65 m. The vertical data follow a similar trend for all directions, indicating radially symmetric uplift. The horizontal data also appear to be similar in all directions but only if measurements near Ricettone (gray circles at about 3.6 km) are neglected. The inset also shows the location of Pozzuoli (star), the inferred center of uplift lies about 1 km to the east.

most analyses of the 1982–1984 vertical movements refer to deformation between June 1982 and June 1983 (Figure 7 in this paper and Figure 5 in the study by *Bianchi et al.* [1987]). The June 1982–1983 data may thus refer to changes between January 1982 and June 1983 but assumed from the tide-gauge data that no movement had occurred between January and June 1982. To assist comparison with previous studies of vertical movement, this paper uses the June 1982 to June 1983 data set in the study by *Bianchi et al.* [1987].

4.3. Data for Horizontal Deformation

[21] Although vertical movements during the 1982–1984 unrest have been analyzed for several ranges of time interval (Table 1), only two data sets, *A* and *B*, are available for horizontal movements. They are distinguished by the time intervals between measurements and by the form in which the data are presented. Data set *A* [*Berrino et al.*, 1984; *Bianchi et al.*, 1987] compares measurements in June 1983

Figure 6. Comparison of observed (circles) and expected horizontal movements applying sill models to the September 1980 to September 1983 data set. Measurements show displacements between sleceted stations to the west, east, and north of station A1 (see Figure 2b for locations). The model data are triangles from the rectangular sill in homogeneous crust of *Dvorak and Berrino* [1991], squares from the penny-shaped sill in homogeneous crust from *Battaglia et al.* [2006], and diamonds from the penny-shaped sill in layered crust from *Amoruso et al.* [2008]. The distances are those of the further station from the center of uplift. In order of increasing distance from the center, the pairs of measuring stations are westward, A1–A2, A2–A3, A3–A4, and A4–A5; eastward, A1–S (movement ~0.1 m), S–C1, and C1–C3; and northward, B1–B2 and B2–B5 (see Figure 2).

with reference positions in January 1982 and provides the horizontal displacement of 19 measuring stations relative to the center of uplift (Figure 2). Data set *B* [*Dvorak and Berrino*, 1991] compares measurements in September 1983 with reference positions in September 1980 and provides the horizontal displacements between 13 pairs of stations, most of which are not referenced to the center of uplift (Figure 2).

[22] Previous sill models have used data set *B* [*Dvorak and Berrino*, 1991; *Battaglia et al.*, 2006; *Amoruso et al.*, 2008]. This paper uses data set *A* because it covers the same time period that will be used to investigate vertical movements, and compared with set *B*, it contains more horizontal measurements and is the only set that includes the key Ricettone data described below. It also provides an additional test of the sill model developed from set *B*.

4.4. Deformation Between June 1982 and June 1983

[23] For the interval June 1982 to June 1983, *Bianchi et al.* [1987] reported similar patterns of deformation (vertical and horizontal) along all three measuring lines, centered upon a coastal station about 800 m east of the old town of Pozzuoli (Figures 2 and 7). Their analysis, as well as subsequent studies, has thus assumed a radial symmetry for deformation in Campi Flegrei. However, although the pattern of vertical deformation is radially symmetric, such symmetry for horizontal deformation is obtained only by discarding measurements near Ricettone (about 3.6–3.8 km north of Pozzuoli), where movements were about half of the values at equivalent distances from Pozzuoli to the WNW and ESE (12–13 cm compared with about 23 cm; Figure 7). No objective criteria have been presented to show that the Ricettone data are incorrect; it thus appears that the data have been rejected on the assumption that the horizontal deformation should be radially symmetric. An alternative view is that, rather than being anomalous, the Ricettone data indicate a nonsymmetrical pattern of horizontal deformation, with greater horizontal extension occurring along the WNW-ESE directions compared with the approximately N-S line between Pozzuoli and Ricettone. The following analysis therefore relaxes the starting assumption that the Ricettone data are anomalous.

4.5. Quantitative Constraints on Deformation Models

[24] Constraints on deformation models can be obtained from evaluations of the overpressure required to drive an intrusion; of crustal rheology and structure; and of the size, shape, and location of the deforming source. These constraints are applied to Campi Flegrei in Appendix A. The results indicate that (1) crustal deformation can be modeled in terms of the behavior of a homogeneous, elastic medium with a rigidity μ of between 5 and 8.5 GPa; (2) the pressure source driving deformation lies at depths of less than 4 km and has a characteristic thickness much less than 1 km; (3) maximum source overpressures must be on the order of MPa; and (4) any ring faults around the caldera have not significantly affected the pattern of surface deformation.

4.6. Applying the Sill Model of *Fialko et al.* [2001]

[25] Given the above constraints, the 1982–1984 uplift has been modeled assuming that deformation was controlled by a uniformly pressurized sill, approximated to a hori-

zontal, penny-shaped crack, embedded in a homogeneous, elastic crust [*Fialko et al.*, 2001]. First estimates of the maximum change in uplift, $\Delta U_{\nu,\max}$ commonly use the analytical solution in the study by *Fialko et al.* [2001]:

$$\Delta U_{\nu,\max} = \frac{4(1-\nu)}{\pi}\frac{\Delta P}{\mu}\left(\frac{a}{f}\right)^2 a, \tag{1}$$

where ΔP is the source overpressure, μ and ν are the modulus of rigidity and Poisson's ratio of the crust, and a and f are the radius and depth of the sill.

[26] Equation (1) is valid for $a/f \leq 0.1$. However, for $1/2 \leq a/f \leq 4/3$, we can introduce a new approximation to the numerical results of *Fialko et al.* [2001] that yields (Figure 8):

$$\Delta U_{\nu,\max} \approx \frac{8(1-\nu)}{3\pi}\frac{\Delta P}{\mu}\left(\frac{a}{f}\right)^{\frac{5}{3}} a. \tag{2}$$

Setting $\nu = 0.25$, $\mu = 5$–8.5 GPa, $\Delta P < 10$ MPa, and, to simulate the maximum uplift for each episode of unrest, also $\Delta U_{\nu,\max} = 1.75$ m, equation (1) yields unreasonable source depths of $\sim 10^3$ km or more for $a/f \leq 0.1$. In contrast, equation (2) gives source depths on the order of kilometers for a/f between 1/2 and 4/3. The full numerical analysis is thus expected to indicate that deformation has been caused by the pressurization of a sill with a final radius comparable to its depth.

5. Model Results for a Pressurized Sill Deforming Campi Flegrei

5.1. Patterns of Vertical Deformation

[27] Figure 9 compares model trends with observation for vertical deformation during June 1982 to June 1983 ($\Delta U_{\nu,\max} = 0.65$ m). Visually reasonable fits are found for depths of 2.5–3 km. Detailed simulations within this depth range yield best fit results, based on χ^2 testing (Table 2), of a source with radius 2.0–2.1 km at corresponding depths of 3–2.75 km and values of $(1-\nu)\Delta P/\mu$ of 5.7–7.5 × 10^{-4}. The implied values for a/f lie between 2/3 and 3/4, which are within the range of validity for equation (2).

[28] During the 1982–1984 uplift, the pattern of vertical deformation showed that the limit of significant uplift was persistently recorded about 5 km from Pozzuoli, independent of the total amount of uplift that had occurred (Figure 5). Apparently, the sill initially spread to a given distance and then evolved primarily by thickening. This condition is consistent with observations of exhumed magmatic sills and laccoliths [*Paige*, 1913; *Pollard and Johnson*, 1973; *Jackson and Pollard*, 1988; *Zenzri and Keer*, 2001; *McCaffrey and Cruden*, 2002]; it may also be consistent with the swelling of aqueous sills, although this has yet to be confirmed independently. In either case, the pattern is consistent with uplift being driven by an increasing overpressure within a sill of constant radius (Figure 5). For such circumstances, the final values of $\Delta P/\mu$ can be estimated from $(\Delta P_{\text{subset}}/\mu)(\Delta U_{z,\max,\text{ final}}/\Delta U_{z,\max,\text{ subset}})$, where ΔP_{subset} and $\Delta U_{z,\max,\text{ subset}}$ here refer to the overpressure and uplift associated with the interval of our analysis (June 1982 to June 1983).

[29] Two values can be chosen for the net final uplift: either the 1.8 m when uplift ceased or the 1.3 m remaining
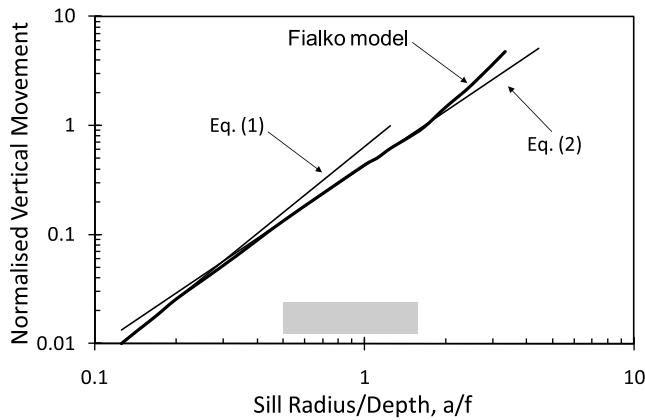
Figure 8. Comparison of results from the penny-shaped source model of *Fialko et al.* [2001] and from equations (1) and (2). The shaded box shows the range of *a/f* for which equation (2) is considered to be valid. Equation (1) is valid for *a/f* less than about 0.1. The normalized vertical movement is given by $(\Delta U_{v,max}/a)\,(\mu/\Delta P)\,[1/2(1-\nu)]$.

after the caldera had returned to its state of equilibrium rate of subsidence (section 2). Applying limiting values of 1.3–1.8 m for $\Delta U_{z,max,\,final}$, the final values of $(1-\nu)\,\Delta P/\mu$ at the end of uplift in December 1984 can be estimated at between 1.1×10^{-3} and 1.6×10^{-3} for a depth of 2.75 km and between 1.5×10^{-3} and 2.1×10^{-3} for a depth of 3 km. Setting $\nu = 0.25$ and $\mu = 5$ GPa, the corresponding ranges of final overpressure in the sill are 7.5–10.5 and 10.0–14.0 MPa; for $\mu = 8.5$ GPa, they become 12.5–17.6 MPa and 17.0–23.8 MPa (see Appendix A for the choice of μ). Given the initial constraint that overpressures should be less than 10 MPa, therefore, the preferred solution is for sill emplacement at a depth of about 2.75 km in a crust with bulk rigidity closer to 5 than to 8.5 GPa.

[30] The interpretation of a thickening sill further suggests that pressurization occurred because of the influx of new material rather than the expansion of fluid already at the depth of the future pressure source (e.g., by the heating of pore fluids). The initial ascent of fluid, however, has not been recorded by the deformation data, which are associated only with changes within a sill-like pressure source. Hence,
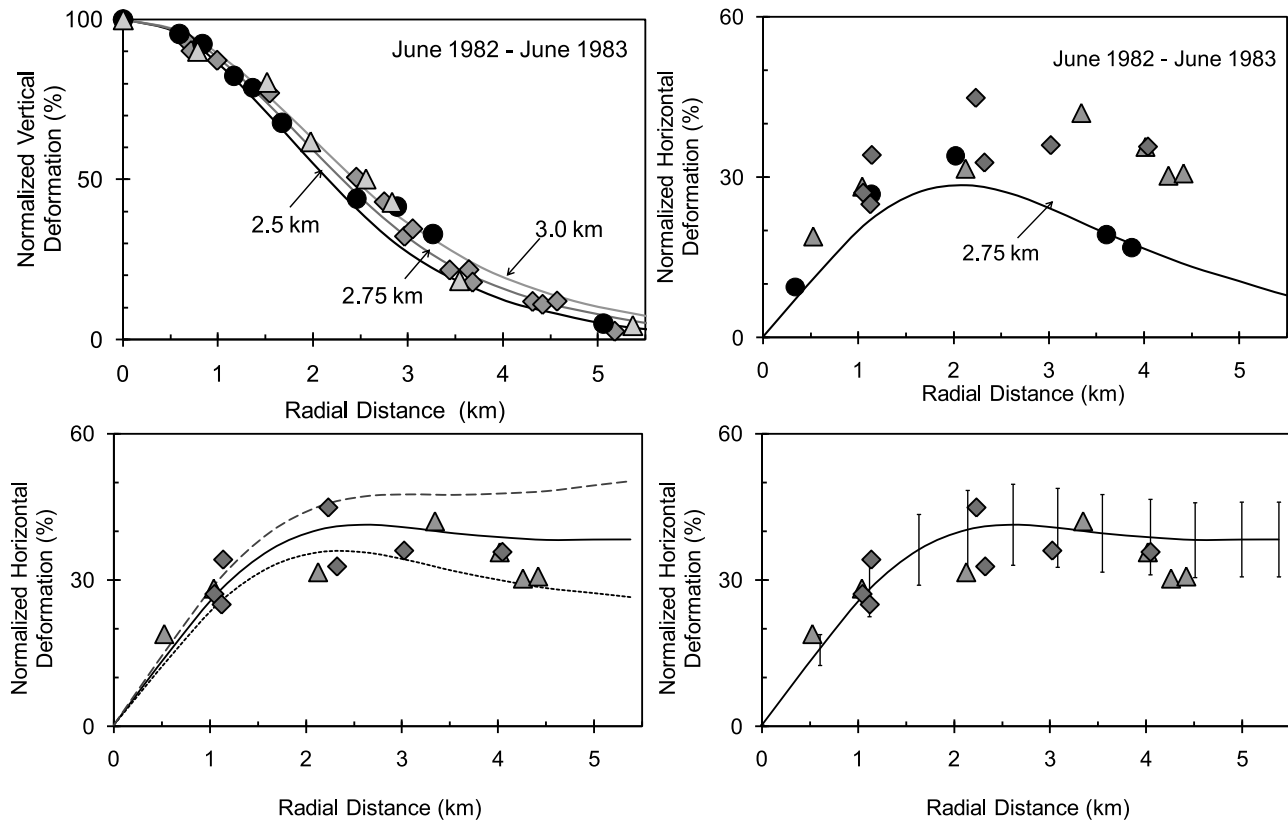

Figure 9. Comparison between (top left) vertical and (top right) horizontal deformation data and results (curve) from best fit sill model (fitted using the vertical data alone). The three measuring lines are (see also Figures 2 and 7) from Pozzuoli westward to Baia and Miseno (diamonds), from Pozzuoli eastwards to Bagnoli and Posillipo (triangles) and from Pozzuoli northward to Ricettone (circles). The model agrees with the Pozzuoli-Ricettone data, but underestimates the horizontal deformation along the other two lines. The horizontal pattern can be reproduced by adding a constant horizontal tensile strain to the Pozzuoli-Baia and Pozzuoli-Bagnoli lines. (bottom left) The curves show the addition of strains of 3.4×10^{-5} (lower, dotted), 5.6×10^{-5} (solid, middle), and 7.8×10^{-5} (dashed, upper). All the points lie within 22% of the values from the curve with (bottom right) an additional strain of 5.6×10^{-5}. Note that, because strain is being added both to the west and east of Pozzuoli, it shows a mirror symmetry across an approximately N-S line through the center of deformation (see Figure 12).

Table 2. Results of a χ^2 Goodness of Fit Test [*Bevington and Robinson*, 2003] for the Penny-Shaped Source Model [*Fialko et al.*, 2001] Applied to Vertical Deformation Across Campi Flegrei During June 1982 to June 1983 ($\Delta U_{v,\max} = 0.65$ m)[a]

Radius, a (km)	χ^2
2.50 km Depth	
1.39	8.28
1.56	5.76
1.67	4.47
1.92	2.88
2.50	*1.65*
2.75 km Depth	
1.38	4.59
1.53	3.60
1.72	2.70
1.83	2.15
2.12	*1.26*
3.00 km Depth	
1.50	2.47
1.67	1.81
1.88	1.47
2.00	*1.35*
2.31	2.28

[a]For a given depth of sill, the test identifies the value of sill radius that provides the pattern of surface deformation that fits most closely to the values obtained at stations of the leveling network. Lower values of χ^2 correspond to better fits. The lowest, and preferred, χ^2 value for each depth is significant at a confidence level greater than 99% (shown by italic font). To test the penny-shaped model, the analysis has been applied only to vertical deformation because the pattern of horizontal deformation cannot be attributed to a pressurized sill alone (see main text).

the effect of the initial ascent must have been (1) too small to be recorded because of a small magnitude or because it occurred too quickly to have been distinguished from sill growth during the measurement intervals or (2) shielded from surface detection by subsurface structures.

[31] The change in volume ΔV for a penny-shaped source can be estimated from equation (2) as $(8/3)$ $(1 - \nu)$ $(\Delta P/\mu)$ a^3. The preferred solution for deformation (sill depth and radius of 2.75 and 2.1 km; $(1 - \nu)$ $\Delta P/\mu$ between 1.1×10^{-3} and 1.6×10^{-3}) thus yields a final volume for new material into the sill of about 0.03–0.04 km^3, which happens to be within the range of common volumes (0.01–0.1 km^3) for post-NYT eruptions. It also indicates a mean thickness ($\Delta V/\pi a^2$) for the sill of about 3 m.

5.2. Patterns of Horizontal Deformation

[32] Figure 9 shows the pattern of horizontal deformation during June 1982 to June 1983. To distances of about 1.5 km from the reference station, the data along all three measuring lines appear to follow a similar trend. However, at distances between 2 and 4.5 km, deformation along the coastal lines (toward Baia and toward Bagnoli) remains high at 30%–45% normalized units (percentage of the maximum vertical deformation); along the northern line, in contrast, measurements near Ricettone (at distances of 3.6–3.9 km) record movements of only 17%–19% normalized units.

[33] Figure 9 also shows the pattern of horizontal deformation expected from the best fit sill model selected from the vertical deformation data alone (depth of 2.75 km, radius of 2.1 km). The model trend agrees well with the horizontal

deformation recorded along the northern measuring line from Pozzuoli toward Ricettone. Such a coincidence would be remarkable if the Ricettone data were anomalous, as has conventionally been assumed. A simpler interpretation is that the Ricettone data are valid and that a pressurized sill can account for the observed movements.

[34] In contrast, the horizontal deformation along the coastal measuring lines tends to be larger than that expected from the sill model. The discrepancy between observed and model values increases with distance, from about 5%–10% normalized units at a distance of 1 km to about 15%–20% normalized units at 4 km (Figure 9). Indeed, if a linear increase in displacement with distance (i.e., a constant strain) is added to the pattern expected from the sill, the total deformation pattern approximates observations along both coastal lines (Figure 9). Apparently, therefore, the approximately E-W strain in Campi Flegrei has been controlled by both a sill and a second source that has yet to be identified.

[35] The orientation of the additional strain coincides with the tectonic ESE-WNW extension inferred to have operated in the Campanian region during the Holocene [*Milia et al.*, 2009]. In addition, paleoseismic analyses [*Roberts*, 2006; *Papanikolaou and Roberts*, 2007] indicate that the Apennine mountain chain is extending SW at mean strain rates of about 10^{-4} ka^{-1} and about 2.5×10^{-5} ka^{-1} for the central and southern Apennines, respectively (Figure 3). Campi Flegrei is separated from the two Apennine sections by the major NE-SW faults bounding the Campanian Plain near mounts Massico and Sorrento (Figure 3). The section of crust containing Campi Flegrei may thus be shearing along its northwestern and southeastern boundaries, a condition that would favor a net tension at approximately 45° to the direction of shearing [*Jaeger*, 1969], that is, approximately E-W. The additional broad E-W strain at Campi Flegrei may thus be a result of external regional movements (1) providing the required strain or (2) determining the orientation of local structures that, in turn, favor an approximately E-W strain.

5.3. Source of Additional Horizontal Strain

[36] The source of additional strain must satisfy the following two requirements.

[37] 1. It must have operated during the period of observation; otherwise, it would not appear when comparing changes in displacement with time.

[38] 2. It is unlikely to have operated much beyond the time interval of unrest. Bulk failure of the crust in tension is expected at maximum strains given by the ratio tensile strength/Young's modulus (σ_T/E). For a Poisson's ratio of 0.25, $E = 2.5\mu$ [*Jaeger*, 1969], and so, crustal rigidities on the order of 1–10 GPa (Appendix A) indicate values of E of similar magnitudes. Hence, with a σ_T of ~10 MPa or less and a strain rate of 5.6×10^{-5} a^{-1}, conditions for bulk failure should recur at intervals of about 10 years or less. Such failure would trigger significant seismic activity. However, since the last eruption in 1538, the first episode of elevated seismicity to have been recorded in Campi Flegrei appears to have been that associated with the 1968–1972 unrest, after an interval of 4 centuries. Accordingly, the additional strain cannot have increased at the estimated rate for a significant amount of time beyond the episodes of unrest.
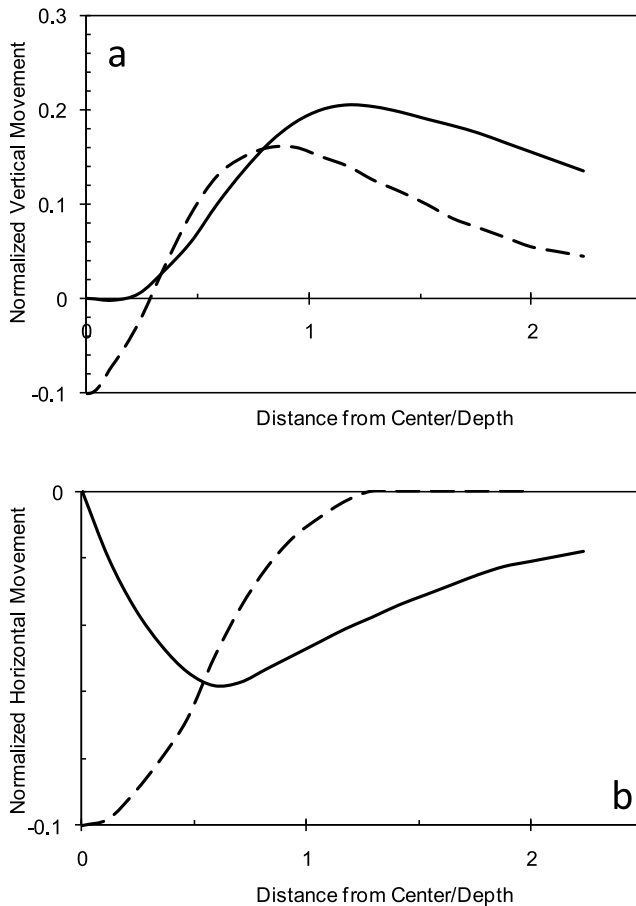
Figure 10. Normalized vertical (dashed curve) and horizontal (solid curve) deformation due to a vertical, fluid-filled point fracture (a) perpendicular to and (b) along the strike of the fracture. The normalized vertical and horizontal movements are given by the actual movements divided by $(1 - \nu)\,(\Delta P/\mu)\,(A/\pi)^{3/2}\,(1/f)^2$, where A is the surface area of the fracture (after *Davis* [1983], *Okada* [1992], and *Lisowski* [2007]).

[39] A third requirement follows if it is assumed that the fluid in the pressurized sill, whether magma or an aqueous fluid, was transported upward from deeper levels. In this case, the source of additional deformation must have affected either shallow depths alone or the whole crust; it cannot have operated only at large depths. The constraint follows because the upward transport of fluid is associated not only with an increase in pressure at shallow level (where the sill is forming) but also with a decrease in pressure in the zone from which the fluid is rising. Hence, the additional source of pressure cannot be associated only with the deeper source of the moving fluid (in which pressure is decreasing). Instead, it must either supplement the growth of the sill in the shallow zone of increasing pressure or be related to an external mechanism that affects the crust independently of the transport of fluids.

[40] The three requirements together suggest that the source of additional horizontal strain is the result either of pressure changes in the shallow crust that are controlled by the transport of fluid or of short-term tectonic changes. Compared with tectonic controls, conditions in the shallow

system can be more tightly constrained and so will be investigated first.

5.4. Shallow Sources of Additional Horizontal Deformation

[41] An extensional E-W stress field would favor upward fluid movement through a vertical pathway elongated N-S (e.g., a dike-like geometry or a collection of fractures for the respective transport of magma or aqueous fluids). The horizontal deformation due to such a body is greater perpendicular to its strike than along the strike direction [*Davis*, 1983; *Lisowski*, 2007]. A pressurized N-S pathway feeding the sill is thus a natural candidate for producing the additional horizontal E-W movements. However, as mentioned in section 5.1, surface deformation due to such a feeder was not recorded before sill growth. It is therefore unlikely that the feeder could have produced detectable surface deformation during sill growth.

[42] On the other hand, a N-S protrusion extending above the sill could have contributed to the observed deformation. To avoid distorting the radial symmetry of the sill's vertical deformation, the protrusion must be both much smaller than the sill [*Lisowski*, 2007] and located near the center of the sill's upper surface. In this case, the deforming source can be modeled as a penny-shaped sill [*Fialko et al.*, 2001] with, projecting upward from its center, a vertical, fluid-filled tabular body with a maximum dimension much shorter than (about one tenth or less) the sill's diameter. Given that the sill's diameter is less than its depth below the surface, it follows that the dimensions of the protrusion must also be much smaller than its depth and, hence, can be described as a "point source" [*Okada*, 1992; *Lisowski*, 2007]. The fluid-filled tabular body is thus referred to as a fluid-filled point fracture.

5.5. Deformation due to a Pressurized Sill With Upward Vertical Protrusion

[43] The normalized deformation field due to a vertical, fluid-filled point fracture is illustrated in Figure 10 for directions parallel and perpendicular to the strike. The results of combining this deformation field with that of the sill are shown in Figure 11 for depths of 2.5, 2.75, and 3.0 km, each for three different values for the ratio of depth to sill radius (1.3, 1.5, and 1.7). In all cases, the point fracture is oriented approximately N-S along the Pozzuoli-Ricettone line. Compared with deformation from a sill alone, the effect of adding the fluid-filled point fracture tends to increase the vertical and horizontal deformation perpendicular to the strike but to reduce deformation along the strike. Good solutions are seen for a depth of 2.75 km and a sill radius between 1.6 and 1.8 km. In the approximately E-W direction, excellent agreement is obtained between modeled and observed horizontal movements, whereas the modeled vertical deformation marginally overestimates observed values (Figure 11). In the N-S direction, the model results follow the observed trends but underestimate both vertical and horizontal displacements (Figure 11). Nevertheless, the combined results show a closer overall fit to observation than those from the penny-shaped sill alone (Figure 7).

[44] The solutions in Figure 11 were obtained by associating a movement of 0.06 m induced by the fluid-filled
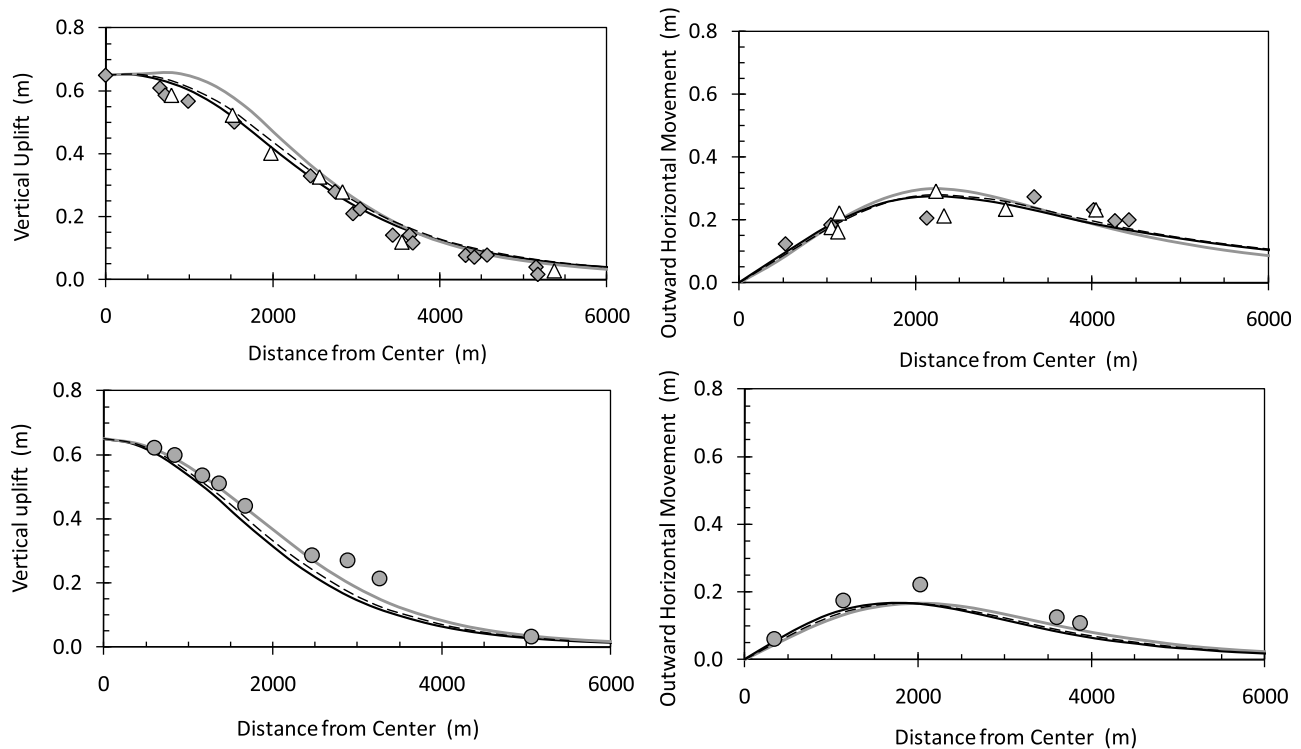
Figure 11. Vertical and horizontal displacements due to a combined penny-shaped sill and vertical, fluid-filled point fracture at a depth of 2.75 km. The center of deformation is shown by the triangle in Figure 2a. The vertical fracture is trending approximately N-S on the Pozzuoli-Ricettone line. The top panels refer to deformation between Pozzuoli and (a) Baia to the west (diamonds) and (b) Bagnoli to the east (triangles). The bottom panels refer to the Pozzuoli-Ricettone-Quarto line. In all plots, the three trends define different ratios of sill depth to radius: 1.3 (solid black curve), 1.5 (dashed black curve), and 1.7 (solid gray curve).

point fracture with 0.1 normalized units in Figure 10. Following the approach in the study by *Okada* [1992] and *Lisowski* [2007], these normalized units are given by the appropriate surface deformation divided by $(1 - \nu) (\Delta P/\mu)$ $(A/\pi)^{3/2} (1/f)^2$, where A is the surface area of the point fracture; it thus follows that the solutions require $(1 - \nu)$ $(\Delta P/\mu) (A/\pi)^{3/2} (1/f)^2 = 0.06/0.1 = 0.6$. Because the sill and point fracture are combined, the overpressures in each must be the same. Applied to the results in Figure 11, as the sill radius increases from 1.6 to 1.8 km, the value of $(1 - \nu) \Delta P/\mu$ for June 1982 to June 1983 ($\Delta U_{z,\max} = 0.65$ m) decreases from 1.2×10^{-3} to 0.7×10^{-3}. Hence, applying a notional value of 10^{-3} and setting $f = 2.75$ km, the indicated value of A is 8.6 km^2. However, to accommodate the assumption of a point source, the area of the protrusion must be less than 0.075 km^2 (i.e., $<(f/10)^2$). The results are thus inconsistent with the model's assumptions and so must be discarded.

5.6. Deformation due to Tectonic Extension

[45] Given the inconsistent results from the combined sill and fluid-filled point fracture (Figure 11), the preferred source for the additional horizontal strain is an increase in tectonic extension along an approximately E-W direction. The data in Figure 9 are consistent with a constant increase in strain by $(5.6 \pm 2.2) \times 10^{-5}$ between June 1982 and 1983. The associated rate of applied stress is E times the strain rate. Setting $E = 2.5\mu$ and, from the best fit sill results, $\mu = 5$

GPa for the upper crust (in which deformation is observed), the rate of increase in stress can be estimated at 0.7 ± 0.3 MPa a^{-1}.

[46] The estimated stress rates are similar to the value implied by *Bianchi et al.* [1987] for the 1968–1972 unrest. Thus, *Bianchi et al.* [1987] noted that an increase in tensile tectonic stress on the order of 1 MPa enhanced model fits to deformation between June 1970 and September 1972 (the interval for which data were available). The corresponding mean stress rate would have been 0.4 MPa a^{-1}. An external stress field was a minor part of the analysis in the study by *Bianchi et al.* [1987], which left its influence and orientation as a matter of speculation. Nevertheless, the similarity of the results here for 1982–1984 suggests that external tension may have operated during both of the uplifts between 1968 and 1984.

6. Discussion

[47] Data set A for the 1982–1984 unrest is consistent with deformation being caused by the emplacement of a sill about 2.75 km below the surface, within a background field of horizontal tension. The sill has a radius and mean thickness of about 2.1 km and 3 m, respectively. The depth of emplacement lies within 13% of the preferred depths of 3 and 2.6 km from the homogeneous crustal models of *Dvorak and Berrino* [1991] and *Battaglia et al.* [2006], as

well as the depth of 3.1 km from the layered crustal model of *Amoruso et al.* [2008], all of which were determined using data set *B* for the unrest. An emplacement depth of around 2.6–3.1 km thus remains a robust solution for both data sets and insensitive to the rheological models that have been chosen for the overlying crust.

[48] Introduction of regional extension provides a simple explanation for the nonradial symmetry of the horizontal movements and represents a first-order improvement on deformation studies that neglect the influence of a regional stress field. The extension occurred at a mean rate of tensional strain of about 5.6×10^{-5} a^{-1}, with an orientation consistent with the ESE-WNW extension of the Holocene regional stress field [*Milia et al.*, 2009].

[49] The results yield constraints on the number of controlling-stress components, their geometry, orientation, and magnitude. Moreover, when combined with supplementary arguments, they can also constrain whether the material in the sill was magma or another fluid, and whether the tectonic-related stress was an active or passive component in triggering unrest.

6.1. Nature of the Deforming Fluids

[50] Combining gravity and deformation changes during unrest provides the most direct remote method for identifying the nature of the material causing deformation [*Rymer*, 1995]. Using this approach, *Battaglia et al.* [2006] and *Amoruso et al.* [2008] inferred respective mean densities of 630 ± 480 and 2500 kg m^{-3} for new material in the sill. The values embrace the densities expected for an aqueous-gas mixture and much denser magma. The difference is due to the density structure assumed for the overlying crust. Hence, the gravity changes will yield ambiguous results until appropriate new data are available on the density distribution of the upper crust in Campi Flegrei.

[51] However, alternative constraints are available from the longer-term pattern of deformation and the volumes of material involved. These are

[52] 1. Since Roman times, episodes of unrest has left a permanent net uplift at Pozzuoli of about 33 m (Figure 4) [*Bellucci et al.*, 2006]. Such uplift is consistent with the permanent emplacement of new material in the crust, for which the simpler mechanism is the injection and solidification of magma.

[53] 2. The final volume of the deforming sill is estimated at 0.03–0.04 km^3. This value is within the range of common volumes (0.01–0.1 km^3) erupted since the NYT caldera was formed. The similarity would be a remarkable coincidence if the intruding and erupting fluids were different. Again, the simpler interpretation is that magma escapes from a deeper reservoir in batches of ~0.01–0.1 km^3 and that these batches either form intrusions or feed eruptions.

[54] 3. At Pozzuoli, the 1982–1984 uplift of 1.8 m was followed by a net subsidence of 0.5 m, yielding a permanent uplift of 1.3 m (Figure 5). This suggests the action of two components, for the permanent and temporary uplift; hence, if the first is attributed to magma emplacement, then the second can be attributed to temporary pressure changes in aquifers caused by the magmatic intrusion.

[55] Together, these constraints favor magma as the primary fluid driving uplift at Campi Flegrei. Assuming this to be the case, the sill will lose heat to the surrounding crust by

conduction and the convective flow of any crustal fluids. The maximum solidification time can be estimated assuming conductive heat loss alone, for which the time scale for solidification is Bh^2/κ [*Jaeger*, 1961; *Rubin*, 1995], where B lies between 1 and 4 and the magma's thermal diffusivity k has a minimum value of $\sim 10^{-7}$ m^2 s^{-1} when accounting for the latent heat released during crystallization [*Williams and McBirney*, 1979]. For an average thickness of 3 m, the conductive solidification time is about 3–10 years. The actual solidification time may thus be similar to the duration of uplift, from which it follows that the rate at which a sill thickens may be comparable to the rate of thickening of its solidified margins. To maintain sill growth, therefore, new magma must be fed into the sill between its chilled margins. This feature consistent with a sill spreading to an equilibrium radius and then evolving by thickening. Moreover, a sill emplaced by 1984 would have solidified before the seismic-tomographic studies of the crust were conducted in 2001 [*Zollo et al.*, 2008].

[56] A magmatic interpretation further suggests that uplift since at least Roman times may have been caused by the emplacement of a sequence of sills, apparently centered beneath the vicinity of Pozzuoli [*Bellucci et al.*, 2006]. Thus, if the 1982–1984 unrest is typical of sill emplacement, then the 33 m of permanent uplift in the past 2200 years can be related to the intrusion of as many as 25 sills (33/1.3) with a total volume approaching 1 km^3. During this time, however, only one eruption has occurred, which expelled some 0.02 km^3 of magma in 1538 and produced Monte Nuovo (Figures 1 and 2) [*Di Vito et al.*, 1987].

[57] The preference for intrusion may reflect a general stability condition for the magmatic system, or it may be the result of local structural conditions in the crust. Thus, sill formation may be favored either where ascending batches of magma reach a level of neutral buoyancy [*Ryan*, 1993, 1994] or where lateral discontinuities are already present in the crust [*Thomson*, 2007]. The controlling condition must also account for the eruptions outside the NYT caldera, as well as the lack of eruptions from the southern two thirds of the caldera, which is the zone of deepest collapse [*Cassano and La Torre*, 1987]. If neutral buoyancy is the control, then the location of eruptions outside the caldera can be related to regional tectonic faults and to faults produced during caldera collapse [*Rosi and Sbrana*, 1987; *Zuppetta and Sava*, 1991; *Acocella et al.*, 1999].

[58] However, tectonic faults have also been recognized within the Bay of Pozzuoli and some appear to have fed local eruptions before the NYT event [*Milia et al.*, 2003; *Bruno*, 2004; *Judenherc and Zollo*, 2004]. The lack of offshore eruptions since the NYT may thus indicate instead the influence of new structural conditions that developed during or after caldera formation. An immediate possibility is that collapse itself induced lateral fracturing. If so, then most fracturing would be expected to have occurred beneath the zone of greatest collapse. Accordingly, magma rising to within 2.5–3 km beneath the southern two thirds of the caldera may typically favor emplacement as a sill along an available discontinuity, whereas magma rising from outside the caldera will encounter fewer lateral discontinuities and so more easily reach the surface. Lateral discontinuities can also suppress the deformation expected at the surface during the ascent of magma through a vertical fracture beneath
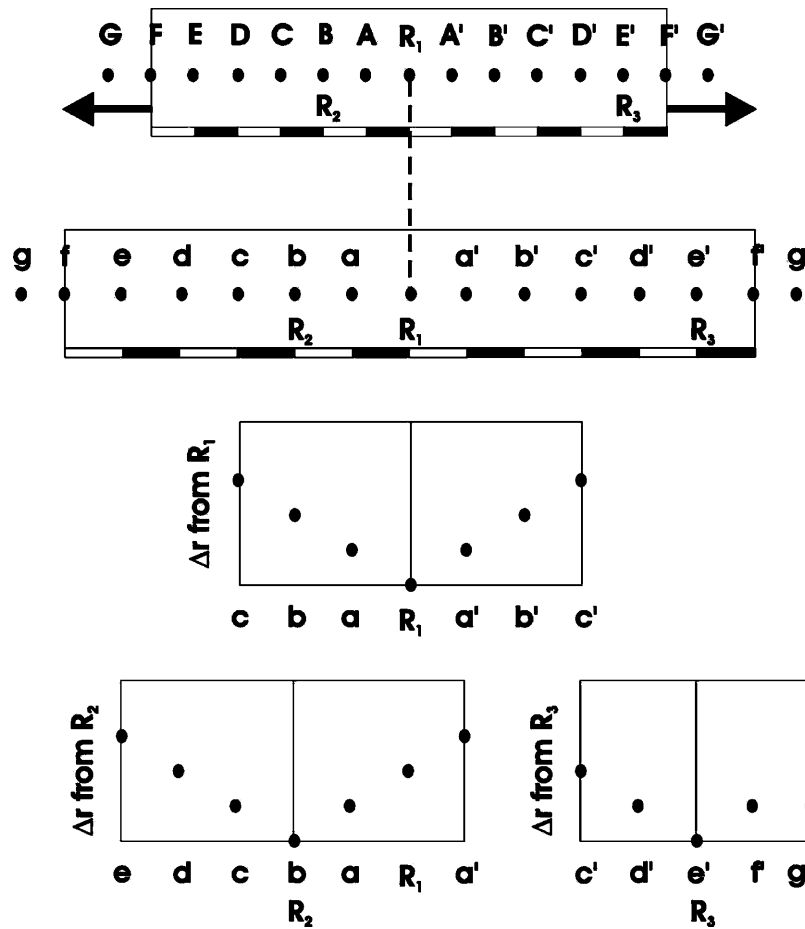
Figure 12. For crust in uniform extension (arrows), the locations of geodetic stations (letters), the same distance apart along the direction of extension will move away from each other by a fixed amount, given by (S/E) times their separation before extension [*Jaeger*, 1969]. Thus, the increase in distance *a-b* compared with *A-B* is the same as that for *d-e* compared with *D-E* or for *c′-d′* compared with *C′-D′*. As a result, any pair of stations the same initial distance, but in opposite directions, from a reference station (such as the pairs *A-A′*, *B-B′*, and *C-C′* about reference station R_1) will appear to move away from the reference station by the same amount (to locations *a-a′*, *b-b′*, and *c-c′*), yielding a symmetrical pattern in the change of distance Δr about the reference station. The same pattern will be observed if a different location is chosen as a reference station (e.g., selecting location *B* as reference station R_2). However, symmetry will break down if locations beyond the zone of stretching crust are also included (e.g., location *G′-g′* from reference station R_3).

them [*Gudmundsson*, 2002, 2003]. Suppression occurs because stresses are locally redirected along the discontinuity rather than being transmitted to the surface. Such a mechanism would favor a lack of surface deformation until the rising magma crossed the discontinuity or until the magma deformed the discontinuity by intruding to form a sill.

[59] Both interpretations suggest that it is not necessary for uplift across Campi Flegrei to have any direct bearing on the potential for eruption. Instead, eruptions may occur when the escape of magma from depth propagates a dike directly to the surface outside the rim of the NYT caldera. In this case, short-term warning of an eruption will occur when the magma approaches the surface. Indeed, the last eruption in 1538 was preceded by uplift centered on the eruption site (3 km west of Pozzuoli) less than 48 hours beforehand [*Parascandola*, 1947]. Such a short warning may thus be common in Campi Flegrei. Emergency management pro-

cedures must therefore be designed to include a response that can be effective in less than a day.

6.2. Regional Tectonics and Unrest in Campi Flegrei

[60] The tectonic component identified for the 1982–1984 uplift appears also to have operated during the 1968–1972 episode [*Bianchi et al.*, 1987] and so may be a common feature of unrest. As argued in section 5.3, it is unlikely that the observed rate of stress increase could have been maintained for more than ~10 years without initiating significant failure on a crustal scale. The absence of such failure suggests that the increase is likely to have developed either during unrest or, at most, only years beforehand.

[61] The additional strain shows a mirror ESE-WNW symmetry across the center of uplift (Figure 9). A first interpretation may thus argue that the regional tension is being focused upon the center by the structure of the Campi

Flegrei caldera. However, regional extension can yield a mirror symmetry in the pattern of local extension independent of where the reference geodetic station is located (Figure 12). Hence, the extension is not necessarily focused on Campi Flegrei, but only appears thus because deformation is being referenced to Pozzuoli. In this case, the crust is expected to have been deforming in a similar manner across the whole Neapolitan volcanic zone, which includes the active centers of Somma-Vesuvius and Ischia, about 22 km to the East and Southwest of Pozzuoli. Neither center has shown significant unrest since the onset of uplift at Campi Flegrei in 1968. Changes in crustal extension, therefore, cannot by themselves determine the onset of unrest at different volcanoes within the Neapolitan volcanic zone; another contributing factor must be either the availability of magma or the potential of magma to ascend to the surface under magmatic conditions alone (e.g., due to overpressure in a deep reservoir).

[62] Extensive zones of magma accumulation have been identified at a depth of about 8 km beneath Campi Flegrei [*Zollo et al.*, 2008] and Somma-Vesuvius [*Auger et al.*, 2001], suggesting that material is usually available for eruption (conditions below Ischia have yet to be determined). The conditions for eruption must therefore lie between the extremes of (1) the passive ascent of magma along fractures that have been opened by tectonic stress alone and (2) the active ascent of pressurized magma without tectonic stretching of the crust. If tectonic stress alone had triggered unrest at Campi Flegrei, then, given the apparent availability of magma beneath the Neapolitan region, at least Somma-Vesuvius would also have been expected to have shown signs of unrest. Such behavior has not been observed. The unrest at Campi Flegrei therefore suggests that, by 1968, the local magmatic system had developed the potential to drive magma ascent given only a small increase in tensile tectonic stress. If verified, this interpretation would identify changes in magmatic conditions, rather than the tectonic stress field, as being the primary control on unrest at Campi Flegrei and its neighboring volcanoes.

7. Conclusions

[63] The pattern of deformation during the 1982–1984 uplift at Campi Flegrei is consistent with the intrusion of 0.03–0.04 km^3 of magma as a sill at a depth of 2.75 km. Tectonic processes were simultaneously straining the crust in a ESE-WNW direction at a rate of about 5.6×10^{-5} a^{-1}. The mean thickness of the sill is about 3 m, so that it is expected to have solidified at the latest within years of unrest. Seismic tomographic studies are thus unlikely to detect sills for two reasons: (1) because their thicknesses are much smaller than the kilometer resolution of the surveys and (2) because they may have solidified by the time post-unrest surveys are carried out.

[64] Although consistent with deformation between June 1982 and June 1983, the general applicability of the interpretations requires a more comprehensive knowledge of changes in tectonic stress across the Campanian region and of the structure and rheology of Campi Flegrei's upper crust. Such knowledge will be improved by enhanced regional geodetic monitoring, and by further investigation of the crust, by remote methods, such as seismic tomography, or by direct studies, such as deep drilling. The new data will not only improve existing models but will also better define the time available for responding to warnings of an eruption.

Appendix A

[65] The starting assumptions for modeling deformation in Campi Flegrei are as follows.

[66] 1. The crust behaves approximately as a continuous medium. The ratio of seismic to potential energy required during deformation is a field measure of the importance of movement along discontinuities (faults large enough to trigger detectable seismicity) compared with the effectively continuous deformation of the crust between the faults. The potential energy, PE, supplied during uplift is $\sim\rho g V \Delta U_{av}$, where ρ and V are the density and volume of deformed crust, ΔU_{av} is the mean vertical uplift, and g is gravitational acceleration. For the 1982–1984 uplift, the zone of deformation can be approximated to a cylinder 5 km in radius and 3 km thick and so, setting ΔU_{av} at 1 m, PE is about 6×10^{15} J. The seismic energy released during the same interval (which involved tens of thousands of events [*Orsi et al.*, 1999]) has been estimated at 5×10^{11} J [*Yokoyama and Nazzaro*, 2002], which is less than 0.01% of the potential energy supplied. Virtually all the energy supplied must therefore have been used to deform the crust as an effectively continuous medium.

[67] 2. The crust behaves approximately as an elastic body. At pressures equivalent to depths of at least 2 km, fracture mechanics experiments indicate that volcanic rocks deform in an elastic brittle manner up to temperatures of at least 600°C [*Rocchi et al.*, 2004; *Smith et al.*, 2009]. Extrapolation of temperature data from boreholes in Campi Flegrei to depths of 3 km suggest that crustal temperatures are expected to be less than about 400°C to depths of about 4 km [*Armienti et al.*, 1983; *Rosi and Sbrana*, 1987]. Given that the crust can be approximated to a continuous medium (Argument 1), therefore, the crust is expected also to behave as an elastic material.

[68] A time-dependent viscoelastic rheology can also be excluded because the time scale for viscous relaxation is $\sim\eta/\mu$ (where η and μ denote viscosity and rigidity [*Jaeger et al.*, 2007]). Hence, for $\mu = 5$ GPa (see section 4), the crust's viscosity would have to be $\leq 2 \times 10^{17}$ Pa s in order for significant viscous relaxation to occur during uplift (~years). Such a viscosity is at least 4 orders of magnitude smaller than realistic values for the upper crust [*Marsh*, 1984], indicating that viscous deformation can be neglected when modeling the 1982–1984 uplift at Campi Flegrei.

[69] 3. The crust can be modeled as a rheologically homogeneous body. Seismic wave velocity provides an estimate of a rock's dynamic rigidity μ_d as it deforms rapidly in response to the passage of seismic waves. A variety of seismic velocities have been proposed for the upper 3 km of Campi Flegrei's crust, from a constant value to steplike increases with depth [*Zollo et al.*, 2008]. Although extreme ranges have been assumed for previous sill models of Campi Flegrei [*Battaglia et al.*, 2006; *Amoruso et al.*, 2008], the results for sill depth and dimension have remained remarkably similar and show an insensitivity to the rheological model employed (section 3). For simplicity, therefore, this

paper assumes a constant velocity model and, following *Aster and Meyer* [1988] and *Zollo et al.* [2008], adopts a characteristic *P* wave velocity ν_p between 2.8 and 3.6 km s^{-1}.

[70] For uplift over years, the static rigidity μ is the more appropriate measure of crustal resistance. Laboratory data indicate that μ/μ_d for crustal materials is commonly between 0.8 and 0.9 [*Mockovčiaková and Pandula*, 2003], so that a nominal value for μ is 0.28 $\rho\nu_p^2$ (compared with $\mu_d = \rho\nu_p^2/3$). Hence, for crustal densities between 2200 and 2400 kg m^{-3} [*Cassano and La Torre*, 1987], the implied value for μ is about 5 GPa for $\nu_p = 2.8$ km s^{-1} and about 8.5 GPa for $\nu_p = 3.6$ km s^{-1}. These values are used here to constrain the rheological state of the crust. For comparison, previous studies at Campi Flegrei have used rigidities in the range of 1.5–23 GPa [e.g., *Bonasia et al.*, 1984; *De Natale et al.*, 1997, 2001; *Troise et al.*, 1997; *Trasatti et al.*, 2005; *Amoruso et al.*, 2008].

[71] 4. Pressure sources occur at depths of 4 km or less and have characteristic dimensions less than 1 km. Seismic events during the 1982–1984 uplift occurred at depths of less than 3.5–4 km [*Aster and Meyer*, 1988; *De Natale et al.*, 1995], which is consistent with a pressure source at such depths or less. In addition, seismic tomographic surveys, with a resolution of about 1 km, have not identified any molten materials to depths of 7.5 km beneath Campi Flegrei [*Zollo et al.*, 2008]. Any magmatic intrusions at depths of less than 7.5 km must therefore have a characteristic thickness (e.g., diameter for an equidimensional body or thickness for a dike or sill) of less than 1 km.

[72] 5. Surface uplift is not constrained by ring faults. The patterns of deformation during 1982–1984 appear to continue smoothly across the rim of the NYT caldera to distances of 5–6 km from Pozzuoli (e.g., Figure 5). This suggests that movements on any ring faults around the NYT caldera have had only a secondary influence on the pattern of uplift. For shallow pressurization, such a pattern is favored by a sill-like, rather than an equidimensional, pressure source [*Folch and Gottsmann*, 2006], thereby favoring a pressurized sill as the deforming source (which is also a geometry that can easily accommodate the size constraints from Argument 4).

References

Acocella, V., F. Salvini, R. Funiciello, and C. Faccenna (1999), The role of transfer structures on volcanic activity at Campi Flegrei (Southern Italy), *J. Volcanol. Geotherm. Res.*, *91*, 123–139.

Amoruso, A., L. Crescentini, and G. Berrino (2008), Simultaneous inversion of deformation and gravity changes in a horizontally layered half-space: Evidences for magma intrusion during the 1982–1984 unrest at Campi Flegrei caldrea (Italy), *Earth Planet. Sci. Lett.*, *272*, 181–188.

Armienti, P., F. Barberi, H. Bizojard, R. Clocchiatti, F. Innocenti, N. Metrich, M. Rosi, and A. Sbrana (1983), The Phlegraean fields: Magma evolution within a shallow chamber, *J. Volcanol. Geotherm. Res.*, *17*, 289–311.

Aster, R. C., and R. P. Meyer (1988), Three-dimensional velocity structure and hypocenter distribution in the Campi Flegrei caldera, Italy, *Tectonophysics*, *149*, 195–218.

Auger, E., P. Gasparini, J. Virieux, and A. Zollo (2001), Seismic evidence of an extended magmatic sill under Mt Vesuvius, *Science*, *294*, 1510–1512.

Avallone, A., A. Zollo, P. Briole, C. Delacourt, and F. Beaudecel (1999), Subsidence of Campi Flegrei (Italy) detected by SAR interferometry, *Geophys. Res. Lett.*, *26*(15), 2303–2306, doi:10.1029/1999GL900497.

Barberi, F., G. Corrado, F. Innocenti, and G. Luongo (1984), Phlegraean Fields 1982–1984: Brief chronicle of a volcano emergency in a densely populated area, *Bull. Volcanol.*, *47*, 175–185.

Barberi, F., E. Cassano, P. La Torre, and A. Sbrana (1991), Structural evolution of Campi Flegrei caldera in light of volcanological and geophysical data, *J. Volcanol. Geotherm. Res.*, *48*, 33–49.

Battaglia, M., C. Troise, F. Obrizzo, F. Pingue, and G. De Natale (2006), Evidence for fluid migration as the source of deformation at Campi Flegrei caldera (Italy), *Geophys. Res. Lett.*, *33*, L01307, doi:10.1029/2005GL024904.

Beauducel, F., G. De Natale, F. Obrizzo, and F. Pingue (2004), 3-D modelling of Campi Flegrei ground deformations: Role of caldera boundary discontinuities, *Pure Appl. Geophys.*, *161*, 1329–1344.

Bellucci, F., J. Woo, C. R. J. Kilburn, and G. Rolandi (2006), Ground deformation at Campi Flegrei, Italy: Implications for hazard assessment, in *Mechanisms of Activity and Unrest at Large Calderas*, edited by C. Troise, G. De Natale, and C. R. J. Kilburn, *Geol. Soc. Spec. Publ.*, 269, 141–158.

Berrino, G., G. Corrado, G. Luongo, and B. Toro (1984), Ground deformation and gravity changes accompanying the 1982 Pozzuoli uplift, *Bull. Volcanol.*, *47*, 187–200.

Bevington, P. R., and D. K. Robinson (2003), *Data Reduction and Error Analysis for the Physical Sciences*, 3rd ed., McGraw-Hill, Boston, Mass.

Bianchi, R., A. Coradini, C. Federico, G. Giberti, P. Lanciano, J. P. Pozzi, G. Sartoris, and R. Scandone (1987), Modeling of surface deformation in volcanic areas: The 1970–1972 and 1982–1984 crises of Campi Flegrei, Italy, *J. Geophys. Res.*, *92*(B13), 14,139–14,150, doi:10.1029/JB092iB13p14139.

Bodnar, R. J., C. Cammatelli, B. De Vivo, A. Lima, H. E. Belkin, and A. Milia (2007), Quantitative model for magma degassing and ground deformation (bradyseism) at Campi Flegrei, Italy: Implications for future eruptions, *Geology*, *35*, 791–794.

Bonasia, V., F. Pingue, and R. Scarpa (1984), A fluid-filled fracture as possible mechanism of ground deformation at Phlegraean Fields, Italy, *Bull. Volcanol.*, *47*, 313–320.

Bruno, P. P. (2004), Structure and evolution of the Bay of Pozzuoli (Italy) using marine seismic reflection data: Implications for collapse of the Campi Flegrei caldera, *Bull. Volcanol.*, *66*, 342–355.

Cassano, E., and P. La Torre (1987), Geophysics, in *Phlegrean Fields*, edited by M. Rosi and A. Sbrana, *Quad. Ric. Sci.*, 114, 103–127.

Cinque, A., G. Rolandi, and V. Zamparelli, (1985), L'Estensione dei depositi marini olocenici nei Campi Flegrei in relazione alla vulcano-tetonica, *Bull. Soc. Geol. Ital.*, *104*, 327–348.

Corrado, G., I. Guerra, A. Lo Bascio, G. Luongo, and R. Rampoldo (1977), Inflation and microearthquake activity of Phlegraean Fields, Italy, *Bull. Volcanol.*, *40*, 169–188.

D'Antonio, M., L. Civetta, G. Orsi, L. Pappalardo, M. Piochi, A. Carandente, S. De Vita, M. A. Di Vito, and R. Isaia (1999), The present state of the magmatic system of the Campi Flegrei caldera based on a reconstruction of its behavior in the past 12 ka, *J. Volcanol. Geotherm. Res.*, *91*, 247–268.

Davis, P. M. (1983), Surface deformation associated with a dipping hydrofracture, *J. Geophys. Res.*, *88*(B7), 5826–5834, doi:10.1029/JB088iB07p05826.

Deino, A. L., G. Orsi, S. de Vita, and M. Piochi (2004), The age of the Neapolitan Yellow Tuff caldera-forming eruption (Campi Flegrei caldera—Italy) assessed by ^{40}Ar/^{39}Ar dating method, *J. Volcanol. Geotherm. Res.*, *133*, 157–170.

De Natale, G., A. Zollo, A. Ferraro, and J. Virieux (1995), Accurate fault mechanism determinations for a 1984 earthquake swarm at Campi Flegrei caldera (Italy) during an unrest episode: Implications for volcanological research, *J. Geophys. Res.*, *100*(B12), 24,167–24,185, doi:10.1029/95JB00749.

De Natale, G., S. M. Petrazzuoli, and F. Pingue (1997), The effect of collapse structures on ground deformations in calderas, *Geophys. Res. Lett.*, *24*(13), 1555–1558, doi:10.1029/97GL01600.

De Natale, G., C. Troise, and F. Pingue (2001), A mechanical fluid-dynamical model for ground movements at Campi Flegrei caldera, *J. Geodyn.*, *32*, 487–517.

De Natale, G., C. Troise, F. Pingue, G. Mastrolorenzo, L. Pappalardo, M. Battaglia, and E. Boschi (2006), The Campi Flegrei Caldera: Unrest mechanisms and hazards, in *Mechanisms of Activity and Unrest at Large Calderas*, edited by C. Troise, G. De Natale, and C. R. J. Kilburn, *Geol. Soc. Spec. Publ.*, 269, 25–46.

De Vivo, B., and A. Lima (2006), A hydrothermal model for ground movements (bradyseism) at Campi Flegrei, Italy, in *Volcanism in the Campania Plain: Vesuvius, Campi Flegrei and Ignimbrites*, edited by B. De Vivo, pp. 289–317, Elsevier, London.

Di Girolamo, P., M. R. Ghiara, L. Lirer, R. Munno, G. Rolandi, and D. Stanzione (1984), Vulcanologia e petrologia dei Campi Flegrei, *Boll. Geol. Soc. Geol. Ital.*, 103, 349–413.

Di Vito, M., L. Lirer, G. Mastrolorenzo, and G. Rolandi (1987), The 1538 Monte Nuovo eruption (Campi Flegrei, Italy), *Bull. Volcanol.*, 49, 608–615.

Di Vito, M. A., R. Isaia, G. Orsi, J. Southon, S. de Vita, M. D'Antonio, L. Pappalardo, and M. Piochi (1999), Volcanism and deformation since 12,000 years at the Campi Flegrei caldera (Italy), *J. Volcanol. Geotherm. Res.*, 91, 221–246.

Dvorak, J., and G. Berrino (1991), Recent ground movement and seismic activity in Campi Flegrei, southern Italy: Episodic growth of a resurgent dome, *J. Geophys. Res.*, 96(B2), 2309–2323, doi:10.1029/90JB02225.

Dvorak, J., and G. Mastrolorenzo (1991), *The Mechanisms of Recent Vertical Crustal Movements in Campi Flegrei Caldera, Southern Italy*, *Spec. Pap. Geol. Soc. Am.*, 263, 54 pp.

Fialko, Y., Y. Kazhan, and M. Simons (2001), Deformation due to a pressurized horizontal circular crack in an elastic half-space, with applications to volcano geodesy, *Geophys. J. Int.*, 146, 181–190.

Folch, A., and J. Gottsmann (2006), Faults and ground uplift at active calderas, in *Mechanisms of Activity and Unrest at Large Calderas*, edited by C. Troise, G. De Natale, and C. R. J. Kilburn, *Geol. Soc. Spec. Publ.*, 269, 109–120.

Gaeta, F. S., F. Peluso, I. Arienzo, D. Castagnolo, G. De Natale, G. Milano, C. Albanese, and D. G. Mita (2003), A physical appraisal of a new aspect of bradyseism: The miniuplifts, *J. Geophys. Res.*, 108(B8), 2363, doi:10.1029/2002JB001913.

Gottsmann, J., H. Rymer, and G. Berrino (2006), Unrest at the Campi Flegrei caldera (Italy): A critical evaluation of source parameters from geodetic data inversion, *J. Volcanol. Geotherm. Res.*, 150(1–3), 132–145.

Gudmundsson, A. (2002), Emplacement and arrest of sheets and dykes in central volcanoes, *J. Volcanol. Geotherm. Res.*, 116, 279–298.

Gudmundsson, A. (2003), Surface stresses associated with arrested dykes in rift zones, *Bull. Volcanol.*, 65, 606–619.

Jackson, M. D., and D. D. Pollard (1988), The laccolith-stock controversy: New results from the southern Henry Mountains, Utah, *Geol. Soc. Am. Bull.*, 100, 117–139.

Jaeger, J. C. (1961), The cooling of irregularly shaped igneous bodies, *Am. J. Sci.*, 259, 721–734.

Jaeger, J. C. (1969), *Elasticity, Fracture and Flow: With Engineering and Geological Applications*, 3rd ed., 276 pp., Chapman and Hall, London.

Jaeger, J. C., N. G. W. Cook, and R. W. Zimmerman (2007), *Fundamentals of Rock Mechanics*, 4th ed., 475 pp., Blackwell, Malden, Mass.

Jellinek, A. M., and D. J. DePaolo (2003), A model for the origin of large silicic magma chambers: precursors of caldera-forming eruptions, *Bull. Volcanol.*, 65, 363–381.

Judenherc, S., and A. Zollo (2004), The Bay of Naples (southern Italy): Constraints on the volcanic structures inferred from a dense seismic survey, *J. Geophys. Res.*, 109, B10312, doi:10.1029/2003JB002876.

Lanari, R., P. Berardino, S. Borgström, C. Del Gaudio, P. De Martino, G. Fornaro, S. Guarino, G. P. Ricciardi, E. Sansosti, and P. Lundgren (2004), The use of IFSAR and classical geodetic techniques for caldera unrest episodes: Application to the Campi Flegrei uplift event of 2000, *J. Volcanol. Geotherm. Res.*, 133, 247–260.

Lima, A., B. De Vivo, F. J. Spera, R. J. Bodnar, A. Milia, C. Nunziata, H. E. Belkin, and C. Cannatelli (2009), Thermodynamic model for uplift and deflation episodes (bradyseism) associated with magmatic-hydrothermal activity at the Campi Flegrei (Italy), *Earth Sci. Rev.*, 97, 44–58.

Lirer, L., G. Luongo, and R. Scandone (1987), On the volcanological evolution of Campi Flegrei, *EOS Trans. AGU*, 68, 226–234.

Lisowski, M. (2007), Analytical volcano deformation source models, in *Volcano Deformation*, edited by D. Dzurisin, pp. 279–304, Springer, Chichester, U. K.

Marsh, B. D. (1984), On the mechanics of caldera resurgence, *J. Geophys. Res.*, 89(B10), 8245–8251.

Mastrolorenzo, G., and L. Pappalardo (2006), Magma degassing and crystallization processes during eruptions of high-risk Neapolitan volcanoes: Evidence of common equilibrium rising processes in alkaline magmas, *Earth Planet. Sci. Lett.*, 250, 164–181.

McCaffrey, K. J. W., and A. R. Cruden (2002), Dimensional data and growth models for intrusions, in *Physical Geology of Subvolcanic Systems—Laccoliths, Sills, and Dykes (LASI): First International Workshop*, *Wiss. Mitt. Inst. Geol.*, vol. 20, edited by C. Breitkreuz, A. Mock, and N. Petford, pp. 37–39, Inst. für Geol., Freiberg, Germany.

Milia, A., M. M. Torrente, M. Russo, and A. Zuppetta (2003), Tectonics and crustal structure of the Campanian continental margin: relationships with volcanism, *Mineral. Petrol.*, 79, 33–47.

Milia, A., E. Turco, P. P. Pierantoni, and A. Schettino (2009), Four-dimensional tectono-stratigraphic evolution of the Southeastern peri-Tyrrhenian Basins (Margin of Calabria, Italy), *Tectonophysics*, 476, 41–56.

Mockovčiaková, A., and B. Pandula (2003), Study of the relation between the static and dynamic moduli of rocks, *Metalurgija*, 42, 37–39.

Okada, Y. (1992), Internal deformation due to shear and tensile faults in a half-space, *Bull. Seismol. Soc. Am.*, 82, 1018–1040.

Orsi, G., M. D'Antonio, S. de Vita, and G. Gallo (1992), The Neapolitan Yellow Tuff, a large-magnitude trachytic phreatoplinian eruption: Eruptive dynamics, magma withdrawal, and caldera collapse, *J. Volcanol. Geotherm. Res.*, 53, 275–287.

Orsi, G., L. Civetta, C. Del Gaudio, S. De Vita, M. A. Di Vito, R. Isaia, S. M. Petrazzuoli, G. P. Ricciardi, and C. Ricco (1999), Short-term ground deformations and seismicity in the resurgent Campi Flegrei Caldera (Italy): An example of active block-resurgence in a densely populated area, *J. Volcanol. Geotherm. Res.*, 91, 415–451.

Paige, S. (1913), The bearing of progressive increase of viscosity during intrusion on the form of laccoliths, *J. Geol.*, 21, 541–549.

Papanikolaou, I. D., and G. P. Roberts (2007), Geometry, kinematics and deformation rates along the active normal fault system in the southern Apennines: Implications for fault growth, *J. Struct. Geol.*, 29, 166–188.

Parascandola, A. (1947), *I Fenomeni Bradisismici del Serapeo di Pozzuoli*, 120 pp., Guida Editore, Naples, Italy.

Pollard, D. D., and A. M. Johnson (1973), Mechanics of growth of some laccolithic intrusions in the Henry Mountains, Utah, II, *Tectonophysics*, 18, 311–354.

Roberts, G. P. (2006), Multi-seismic cycle velocity and strain fields for an active normal fault system, central Italy, *Earth Planet. Sci. Lett.*, 251, 44–51.

Rocchi, V., P. R. Sammonds, and C. R. J. Kilburn (2004), Fracturing of Etnean and Vesuvian rocks at high temperatures and low pressures, *J. Volcanol. Geotherm. Res.*, 132, 137–157.

Rolandi, G., F. Bellucci, M. T. Heizler, H. E. Belkin, and B. De Vivo (2003), Tectonic controls on the genesis of ignimbrites from the Campanian Volcanic Zone, southern Italy, *Mineral. Petrol.*, 79, 3–31.

Rosi, M., and A. Sbrana (1987), *Phlegrean Fields*, *Quad. Ric. Sci.*, 114, 175 pp.

Rosi, M., A. Sbrana, and C. Principe (1983), The Phlegraean Fields: Structural evolution, volcanic history and eruptive mechanisms, *J. Volcanol. Geotherm. Res.*, 17, 273–288.

Rubin, A. M. (1995), Getting granite dikes out of the source region, *J. Geophys. Res.*, 100(B4), 5911–5929, doi:10.1029/94JB02942.

Ryan, M. P. (1993), Neutral buoyancy and the structure of mid-ocean ridge magma reservoirs, *J. Geophys. Res.*, 98(B12), 22,321–22,338, doi:10.1029/93JB02394.

Ryan, M. P. (1994), Neutral-buoyancy controlled magma transport and storage in mid-ocean ridge magma reservoirs and their sheeted dike complex: A summary of basic relationships, in *Magmatic Systems*, edited by M. P. Ryan, pp. 97–135, Academic, San Diego, Calif.

Rymer, H. (1995), Microgravity monitoring, in *Monitoring Active Volcanoes*, edited by W. J. McGuire, C. R. J. Kilburn, and J. B. Murray, pp. 217–247, UCL Press, London.

Saccarotti, G., S. Petrosino, F. Bianco, M. Castellano, D. Galluzzo, M. La Rocca, E. Del Pezzo, L. Zaccarelli, and P. Cusano (2007), Seismicity associated with the 2004–2006 renewed ground uplift at Campi Flegrei caldera, Italy, *Phys. Earth Planet. Inter.*, 165, 14–24.

Scandone, R., F. Bellucci, L. Lirer, and G. Rolandi (1991), The structure of the Campanian Plain and the activity of the Neapolitan volcanoes (Italy), *J. Volcanol. Geotherm. Res.*, 48, 1–31.

Smith, R., P. R. Sammonds, and C. R. J. Kilburn (2009), Fracturing of volcanic systems: Experimental insights into pre-eruptive conditions, *Earth Planet Sci. Lett.*, 280, 211–219, doi:10.1016/j.epsl.2009.01.032.

Thomson, K. (2007), Determining magma flow in sills, dykes and laccoliths and their implications for sill emplacement mechanisms, *Bull. Volcanol.*, 70, 183–201, doi:10.1007/s00445-007-0131-8.

Todesco, M., J. Rutqvist, G. Chiodini, K. Pruess, and C. M. Oldenburg (2004), Modelling of recent volcanic episodes at Phlegrean Fields (Italy): Geochemical variations and ground deformation, *Geothermics*, 33, 531–547.

Trasatti, E., C. Giunchi, and M. Bonafede (2005), Structural and rheological constraints on source depth and overpressure estimates at the Campi Flegrei caldera, Italy, *J. Volcanol. Geotherm. Res.*, *144*, 105–118.

Troise, C., G. DeNatale, F. Pingue, and A. Zollo (1997), A model for earthquake generation during unrest episodes at Campi Flegrei and Rabaul calderas, *Geophys. Res. Lett.*, *24*(13), 1575–1578, doi:10.1029/97GL01477.

Troise, C., G. De Natale, F. Pingue, F. Obrizzo, P. De Martino, U. Tammaro, and E. Boschi (2007), Renewed ground uplift at Campi Flegrei caldera (Italy): New insight on magmatic processes and forecast, *Geophys. Res. Lett.*, *34*, L03301, doi:10.1029/2006GL028545.

Williams, H., and A. R. McBirney (1979), *Volcanology*, 1st ed., 397 pp., Freeman, Cooper, San Francisco, Calif.

Wohletz, K., G. Orsi, and S. de Vita (1995), Eruptive mechanisms of the Neapolitan Yellow Tuff interpreted from stratigraphy, chemical, and granulometric data, *J. Volcanol. Geotherm. Res.*, *67*, 263–290.

Yokoyama, I., and A. Nazzaro (2002), Anomalous crustal movements with low seismic efficiency-Campi Flegrei, Italy and some examples in Japan, *Ann. Geofis.*, *45*, 709–722.

Zenzri, H., and L. M. Keer (2001), Mechanical analyses of the emplacement of laccoliths and lopoliths, *J. Geophys. Res.*, *106*(B7), 13,781–13,792, doi:10.1029/2001JB000319.

Zollo, A., et al. (2003), Evidence for the buried rim of Campi Flegrei caldera from 3-D active seismic imaging, *Geophys. Res. Lett.*, *30*(19), 2002, doi:10.1029/2003GL018173.

Zollo, A., N. Maercklin, M. Vassallo, D. Dello Iacono, J. Virieux, and P. Gasparini (2008), Seismic reflections reveal a massive melt layer feeding Campi Flegrei caldera, *Geophys. Res. Lett.*, *35*, L12306, doi:10.1029/2008GL034242.

Zuppetta, A., and A. Sava (1991), Stress pattern at Campi Flegrei from focal mechanisms of the 1982–1984 earthquakes (Southern Italy), *J. Volcanol. Geotherm. Res.*, *48*, 127–137.

C. R. J. Kilburn and J. Y. L. Woo, Aon Benfield UCL Hazard Research Centre, Department of Earth Sciences, University College London, Gower Street, London WC1E 6BT, UK. (j.woo@ucl.ac.uk)